

HYD 465

BUREAU OF RECLAMATION
HYDRAULIC LABORATORY

UNITED STATES
DEPARTMENT OF THE INTERIOR
BUREAU OF RECLAMATION

**MASTER
FILE COPY**

DO NOT REMOVE FROM THIS FILE

PROGRESS REPORT I--CANAL BANK EROSION DUE TO WIND-GENERATED WATER WAVES

Hydraulic Laboratory Report No. Hyd-465

DIVISION OF ENGINEERING LABORATORIES



OFFICE OF ASSISTANT COMMISSIONER AND CHIEF ENGINEER
DENVER, COLORADO

January 9, 1961

CONTENTS

	<u>Page</u>
Foreword	
Summary	1
Introduction	3
Wind Waves in Canals	3
Review of Literature	3
Wind and Wave Measurements on Bureau of Reclamation Canals	6
Analysis of Data from Bureau of Reclamation Canals	6
Laboratory Study of Wave Erosion	8
Description of Equipment	8
Wave channel	8
Wave generator	9
Description and use of measuring equipment.	10
Description and use of compaction equipment.	12
Calibration of Equipment.	12
Calibration procedure	13
Results and analysis of calibration	14
Waves in Trapezoidal Channels	16
Erosion Tests on Driftwood Canal Soil	18
Soil characteristics.	18
Test procedure	18
Test results	21
Analysis of Results	22
Conclusions.	24
Suggestions for Future Study	24

APPENDIX

Bibliography.	27
List of Symbols	29

CONTENTS--Continued

	<u>Table</u>
Summary of Bureau of Reclamation Canal Data	1
Results of Gradation Analyses	2
Results of Standard Properties Tests	3
Soil Sample Designation	4
Results of Density Measurements	5

	<u>Figure</u>
Wave Erosion in Field and Laboratory--Eden Canal and Laboratory Wave Channel.	1
Dimensionless Graph Showing Relationships Among Fetch, Wind Velocity, Wave Height, Wave Period, Wave Steepness, and Wind Duration in Deep Water.	2
Effective Fetch Length as a Function of Fetch Length and Fetch Width for Rectangular Fetches.	3
Dimensionless Graph of Wave Height as a Function of Wind Velocity and Fetch	4
Dimensionless Graph of Wave Period as a Function of Wind Velocity and Fetch	5
Deep Water Significant Wave Height as a Function of Effective Fetch and Wind Velocity	6
Deep Water Significant Wave Period as a Function of Fetch and Wind Velocity	7
Time Required to Generate Maximum Significant Wave in Deep Water as a Function of Fetch and Wind Velocity	8
Laboratory Wave Channel and Appurtenances--Schematic Sketches	9
Laboratory Equipment--Wave Generator, Filters, and Absorber	10
Laboratory Equipment--Wave Generator and Measuring Equipment for Wave Heights and Lengths	11
Laboratory Equipment--Test Section	12
Laboratory Equipment--Compaction Equipment and Equipment for Measuring Erosion Cross Sections	13
Characteristics of Average Waves.	14
Comparison of Observed with Theoretical Wave Heights	15
Comparison of Observed with Theoretical Wave Celerities.	16
Comparison of Observed with Theoretical Wave Lengths	17
Waves Used in Erosion Tests--Waves 1 and 2	18
Waves Used in Erosion Tests--Waves 3 and 4	19
Wave 5 and Hand-operated Wave Generator.	20
Edge-wave Demonstrations.	21
Edge-wave Relationships.	22
Plasticity Chart--For Laboratory Classification of Fine-grained Soils	23

CONTENTS--Continued

	<u>Figure</u>
Standard Soil Properties Summary	24
Definition Sketch of Erosion in Test Section	25
Run 1-S, Average Erosion Cross Sections for Middle Six Feet of Test Section	26
Run 2-S, Average Erosion Cross Sections for Middle Six Feet of Test Section	27
Run 3-S, Average Erosion Cross Sections for Middle Six Feet of Test Section	28
Run 4-S, Average Erosion Cross Sections for Middle Six Feet of Test Section	29
Run 3-S-A, Average Erosion Cross Sections for Middle Six Feet of Test Section	30
Run 3-S-B, Average Erosion Cross Sections for Middle Six Feet of Test Section	31
Run 5-S, Average Erosion Cross Sections for Middle Six Feet of Test Section	32
Run 2-S-A, Average Erosion Cross Sections for Middle Six Feet of Test Section	33
Wave Erosion Tests--Run 1-S	34
Wave Erosion Tests--Runs 2-S and 3-S	35
Wave Erosion Tests--Runs 4-S and 3-S-A	36
Wave Erosion Tests--Run 3-S-B	37
Wave Erosion Tests--Runs 5-S and 2-S-A	38
Wave Erosion Tests--Runs 4-S and 2-S-A	39
Results of Wetting-Drying, Freezing-Thawing Demonstration	40
Average Volumetric Displacement in Middle Six Feet of Test Section as a Function of Time	41
Average Volumetric Displacement in Middle Six Feet of Test Section as a Function of Time--Semilog Plot	42
Empirical Constants K_1 and K_2 as a Function of Wave Height and Percent Maximum Compaction	43
Volumetric Displacement (\bar{E}) as a Function of Time and Empirical Constants K_1 and K_2	44

FOREWORD

The studies discussed in this report were carried out under the Lower-cost Canal Lining Program, by the Sediment Investigation Unit of the Hydraulic Laboratory, during May to October 1958. All of the laboratory tests were made by W. W. Sayre, with the help of several foreign trainees, under the supervision of E. J. Carlson. The Sediment Investigations Unit is in the Hydraulic Investigations Section which is headed by C. W. Thomas. H. M. Martin is Chief of the Hydraulic Laboratory. P. W. Terrell is Chairman of the Lower-cost Canal Lining Committee.

The field measurements were made by Project Personnel under the direction of the Hydraulic Laboratory. Those projects which furnished field data are Eden Project, Region 4, Tucumcari Project, Region 5, Central Valley Project, Region 2, and the Imperial Irrigation District, California.

The earth material used in the laboratory tests was furnished from Driftwood Canal by the Frenchman-Cambridge Construction Field Division, Missouri River Basin Project, Region 7.

UNITED STATES
DEPARTMENT OF THE INTERIOR
BUREAU OF RECLAMATION

Office of the Assistant Commissioner
and Chief Engineer--Denver
Division of Engineering Laboratories
Hydraulic Laboratory Branch
Denver, Colorado
January 9, 1961

Laboratory Report No. Hyd-465
Compiled by: E. J. Carlson, and
W. W. Sayre
Checked by : E. J. Carlson
Reviewed by: C. W. Thomas
Submitted by: H. M. Martin

**PROGRESS REPORT I--CANAL BANK EROSION DUE
TO WIND-GENERATED WATER WAVES**

SUMMARY

Erosion of earth canal banks by the action of wind-generated water waves has long been a maintenance problem on some irrigation projects. The relationships between wind and waves on one hand and between waves and the resulting erosion on the other hand are complex and involve a large number of variables. Very little has been done in the way of a systematic attempt to solve the problem by separating the effects of the different variables.

The studies covered in this report are divided into two sections:
(1) wind waves in canals and (2) laboratory study of wave erosion.

Measurements of waves, wind velocities, and wind direction have been made on canals of several Bureau of Reclamation projects. These measurements, together with the corresponding canal alignment data and cross-sectional dimensions, have been reported from the field. These data are analyzed in terms of the Sverdrup-Munk-Bretschneider 17/4 parameters. The principal variables involved in the generation of waves in canals are found to be the wind characteristics of velocity and direction, and the fetch characteristics of length, width, and direction. Wind duration and depth of water are generally of lesser importance. The primary dependent variables are wave height and wave period.

The laboratory study involved the calibration of the wave generating equipment in the 70-foot long half-trapezoidal wave channel, Figure 1, and the performance of a series of wave erosion tests on a test embankment simulating a compacted earth canal lining.

The calibration consisted of measuring the wave heights, lengths, celerities, and frequencies for a number of different settings of the wave-generating apparatus. The wave characteristics were varied

17/Refers to reference at end of report.

to cover a range of conditions considered to be typical on the basis of observations made on several irrigation canals. Some observations were made of the characteristics of waves in a trapezoidal channel.

In the wave-erosion tests, a compacted earth test section, measuring 8 feet long and 6 and 1/2 inches thick, was subjected to wave action. The exposed surface of the test section was placed flush with the 1 and 1/2 to 1 sloping sidewall of the channel. The earth material came from the Driftwood Canal in the Frenchman Unit of the Missouri River Basin Project, and is a loessial inorganic clay of low plasticity. Before each test, the embankment was compacted at optimum moisture content to near the maximum dry density as specified by the standard proctor compaction test.

Five different waves were used in these tests. Wave heights were varied from 0.18 to 0.38 foot, trough to crest, and wave frequencies varied from 50 to 75 waves per minute. The stillwater depth was held constant at 1.50 feet. In no case, did complete failure of the test embankment occur. In all tests, the erosion was concentrated near the waterline.

The erosion rate in each test was measured and analysis showed that the volumetric displacement varied approximately with the logarithm of time. The principal variables influencing the erosion rate were the degree of compaction and the wave height. With other factors held constant, the rate of erosion for an embankment compacted to 97 percent of the Proctor maximum dry density was approximately three times that for an embankment compacted to 99 percent of maximum density.

Experiments also demonstrated that if the embankment was permitted to become dry, slaking occurred upon rewetting, and the resistance to erosion was greatly reduced.

INTRODUCTION

The erosion of canal banks by wind-generated waves is a problem which has received little systematic study. As shown by the photograph in Figure 1, which was taken along a straight reach of the Eden Canal in Wyoming after only two seasons of operation, waves cause serious erosion in certain types of soils. Notable among these are the silts, fine sands, and some lean clays. On some projects where this type of erosion has occurred, maintenance forces have met the problem with various degrees of success. The usual method of repair has been to fill the eroded sections with gravel or riprap in order to protect canal banks against further erosion.

Studies performed in the Hydraulic Laboratory of the Bureau of Reclamation 18/, in 1954, on a silty material, indicated that a protective cover must be fine enough to prevent leaching of the base material through it, and that particles on the exposed surface of the protective material must be of sufficient size and weight to resist displacement by wave action.

The results of these studies and the fact that wave erosion has been a continuous source of maintenance on some projects demonstrated the need for a general research program to investigate the problem. Recognizing the need for such a program, the Lower-cost Canal Lining Committee authorized a combined laboratory and field investigation of the problems involved in erosion due to wind waves in canals.

The general aims of this investigation were the development of: (1) criteria for predicting wave characteristics in canals, (2) a laboratory wave flume in which canal waves can be simulated and wave erosion reproduced under controlled conditions, (3) a better understanding of the mechanics of canal bank erosion by waves, (4) a classification of various soil properties with respect to erosion by wave action, (5) methods and design criteria for stabilizing erodible canal banks with respect to wave action, and (6) correlation between laboratory and field studies where possible.

This report deals with the first three of these points and also presents the results of a series of laboratory wave erosion tests on a low plasticity soil from the Driftwood Canal.

WIND WAVES IN CANALS

Review of Literature

Very little research has been done on the subject of wind waves in canals. In recent years, however, an increasing amount of research has been undertaken on the generation of wind waves in oceans, lakes, reservoirs, and laboratory flumes.

Prior to World War II, prediction of wave characteristics was dependent on empirical relations developed by Stevenson 16/, 1874, Gaillard 5/, 1904, Molitor 13/, 1935, and others. Most of these formulas express wave height as a function of wind velocity and fetch. None of them are applicable over a very wide range of wind and fetch conditions.

During the war, investigation of the problem was accelerated due to the interest of the armed forces in connection with amphibious operations. By a combination of theoretical, dimensional, and empirical analysis, Sverdrup and Munk 17/, 1947, derived relationships in which wave characteristics, such as height, length, celerity, and period are expressed as a function of fetch, wind velocity, and wind duration. Fetch is defined as the length of the reach of water over which the wind blows at a particular velocity. Wind duration is defined as the interval of time during which that velocity exists.

Their findings are expressed in the relationships between various dimensionless parameters which combine the wave, wind, and fetch characteristics. Hirschberg 8/, 1949, Johnson 11/, 1950, and others have shown that these parameters may be readily obtained by application of the Buckingham pi-theorem and dimensional analysis.

Although the Sverdrup-Munk relationships were derived for the purpose of predicting the characteristics of ocean waves, Johnson 10/, 1948, 11/, 1950, Bretschneider 2/, 1952, 3/, 1954, 4/, 1958, Sibul 15/, 1955, and others have shown that with minor modifications, the Sverdrup-Munk analysis is also applicable to bodies of water such as lakes, reservoirs, and laboratory flumes where the fetch dimensions are limited. The results of the Sverdrup-Munk analysis as modified by Bretschneider 4/, 1958, are shown in Figure 2.

According to the Sverdrup-Munk analysis, the energy transfer from wind to waves occurs by the push of the wind against the wave crests and by the drag of the wind on the water. The push, or normal pressure is the dominating factor in the early stages of wave growth. The drag force is primarily responsible for the continued growth of waves, even when the wave celerity exceeds the wind velocity. Forces tending to retard the growth of waves are the normal pressure when the wind velocity is less than the wave celerity, and viscous shear, the latter being of negligible importance. Thus, the waves continue to grow until equilibrium is reached between the energy added by shear and that lost by air resistance.

Wave growth is limited by wind velocity and either fetch length or wind duration. In relatively short fetches, maximum wave growth is achieved in a short time and the length of fetch is usually the limiting factor. In very long fetches, wind duration usually controls.

Sverdrup and Munk made another important contribution by introducing the concept of the significant wave. Natural wave trains are seldom uniform with respect to wave height and wave period. The significant wave is defined statistically as the wave having the average height and period of the highest one-third of the total number of waves observed. The Sverdrup-Munk-Bretschneider analysis is based on the concept of the significant wave.

The relationships shown in Figure 2 are all for deep water wave conditions in which the ratio of the wave length to the depth of water L/y is less than 2. When L/y becomes greater than 2, the waves begin to "feel" bottom and the wave height and period are reduced accordingly.

Bretschneider 3/, 1954, has extended the Sverdrup-Munk analysis to cover certain cases of shallow water waves by taking into account energy dissipation due to bottom friction and percolation.

Sibul 15/, 1955, in a series of experiments with wind waves in a laboratory channel demonstrated that the depth begins to affect the wave height when the ratio of the depth to wave height y/H becomes less than 5. A reduction in wave period becomes noticeable when L/y becomes greater than 5. Sibul's experiments included both smooth and rough bottom conditions. Results appeared to be independent of bottom roughness.

Hufft 9/, 1958, in another series of laboratory experiments with wind waves in shallow water, obtained results showing that observed wave heights for L/y ratios up to about 5 do not differ appreciably from those predicted by the Sverdrup-Munk-Bretschneider curves for deepwater conditions. Wave periods, lengths, and celerities were found to be in substantial agreement with their deepwater counterparts over the entire range of experimental conditions which included L/y ratios up to about 7.

Saville 14/, 1954, developed a method for estimating the effect of fetch width in limiting the growth of waves. It is generally recognized that where the width of the fetch is limited by land forms, waves are significantly lower than those that would be expected from the same generating conditions over more open water. It is also known that waves are generated not only in the immediate direction of the wind, but also at various angles with the wind direction. Thus, the wave characteristics measured at a particular point are dependent not only on the energy components in a direction coincident with the wind direction but also on those components from various angles to the wind direction. The actual wave characteristics at the point will result from the summing up of all these components.

Saville used several alternate assumptions in his analysis, but obtained the best results by assuming that the wind effectiveness varies as the cosine of the angle up to 45° on either side of the wind direction, and is zero for angles of greater than 45° . Saville established a graphical relationship in which the ratio of the effective fetch to the actual fetch F_e/F for a rectangular fetch is expressed as a function of the ratio of the fetch width to the actual fetch length W/F .

Wind and Wave Measurements on Bureau of Reclamation Canals

For several years, operation and maintenance personnel on several Bureau of Reclamation projects in addition to the Imperial Irrigation District have been obtaining wind and wave data on canals. Wave height and frequency data were obtained by taking motion pictures of the water surface fluctuations on stationary staff gages. Observation periods ranged from about 10 to 90 seconds. The staff gages were located in the canals about 6 feet away from the bank. Wind velocity measurements were taken simultaneously with the motion pictures by means of an anemometer located on top of the canal bank. Wind direction was also determined. Canal alignment data and the dimensions of the cross section provided the necessary information for determining the length, width, and direction of the fetch.

These data were taken on canals with discharges ranging from 50 cubic feet per second in the West Side Lateral of the Eden project to about 5,000 cubic feet per second in the All-American Canal. Unfortunately, no data were obtained for wind velocities in excess of 30 miles per hour.

The canal data are summarized in Table 1.

Analysis of Data from Bureau of Reclamation Canals

The methods used in analyzing the canal data were basically those of Sverdrup, Munk, and Bretschneider. However, some corrections were made for fetch width, wind direction, and flow velocity in the canal.

When the wind direction coincides with the canal alignment, the fetch dimensions may be described in terms of a long, narrow rectangle of length F , and width W . F is the length of reasonably straight reach of canal immediately upwind from the point of observation; and W is canal width at the water surface. Saville's ¹⁴ method for estimating the effective fetch in rectangular fetches was extended to include values of W/F down to 0.001. The formula

$$F_e = 1.17 F^{1/3} W^{2/3} \quad (1)$$

was found to apply over the range $W/F = 0.001 \rightarrow 0.30$, which includes all of the canal data. F_e is the effective fetch length of a rectangular

fetch, and is used instead of F in estimating the wave height. Results of the fetch width investigations are shown in Figure 3.

When the wind direction is not coincident with the canal alignment, the wind effectiveness is assumed to vary with the cosine of the wind angle according to the formula

$$U_e = U \cos \theta \quad (2)$$

in which U is the wind velocity, and θ the angle between the wind direction and the canal bearing. This assumption appears to be reasonable for deflection angles of less than 45° . For the two cases on Delta-Mendota Canal when the wind blew directly across the canal, F was assumed to equal W .

A correction for flow velocity in the canal was made by modifying Equation 2 to the form

$$U_e = U \cos \theta \pm V \quad (2a)$$

in which V is the average flow velocity in the canal. V is negative when θ is between 0 and 90° , and is positive when θ is between 90° and 180° . This assumption appears to be valid in that the wave characteristics should depend on the relative velocity between wind and water surface.

The modified canal data, in the form of the Sverdrup-Munk-Bretschneider parameters, are plotted in Figures 4 and 5. Although the scatter is considerable, it is not of a greater order of magnitude than the scatter in the data from which the original curves were established. In view of such limitations on the data as the brevity of the observation periods, the transient nature of both wind velocity and wind direction and the total neglect of the effect of wind duration, the correlation appears to be fairly good and the assumptions justified.

Figures 6, 7, and 8, which show wave height, wave period, and wind duration as a function of fetch and wind velocity, were computed and plotted directly from the Sverdrup-Munk-Bretschneider curves in Figure 2.

The lines of constant depth plotted on the wave period graph indicate conservatively the approximate limits to which the deep water wave relationships may be applied. They are based on the limit $L/y = 4$. Computations based on Bretschneider's 3/ analysis show that wave heights for values of L/y up to 4 are at least 90 percent of deep water wave heights for identical wind and fetch

conditions. Sibul's 15/ data show that there is no appreciable change in wave period until L/y reaches 5. Hufft's 9/ experiments show no appreciable reduction in wave height until L/y reaches 5, and no discernable change from the deep water wave period, length or celerity for L/y values as high as 7. L/y values for the canal data computed from the basic deep water wave relationship

$$L = \frac{g}{2\pi} T^2 \quad (3)$$

in no case exceeded 3.8. Consequently, it is believed that in almost all cases, the deep water wave relationships may be used in predicting wave characteristics in canals. Some error may be introduced in cases combining high wind velocities, long fetches, and shallow depths.

The wind duration graph, Figure 8, indicates that in most cases, fetch, rather than wind duration, limits the wave growth in canals. For example, a 30-mile per hour wind blowing along a 10,000-foot fetch would require only 30 minutes to achieve equilibrium conditions with respect to wave growth.

LABORATORY STUDY OF WAVE EROSION

The laboratory phase of the study is divided into the following sections: (1) description of equipment, (2) calibration of equipment, (3) waves in trapezoidal channels, and (4) erosion test on soil from Driftwood Canal.

Description of Equipment

The laboratory equipment consisted essentially of a wave channel, a wave generator, measuring equipment, and equipment for compacting earth into the test section.

Wave channel. The wave channel, Figure 9, was built into an existing 70-foot rectangular flume measuring 8 feet wide and 2 feet deep. A 1-1/2:1 sloping plywood side wall was built into the flume to simulate a canal bank and to permit installation of a 6 and 1/2-inch thick test embankment. This resulted in a half-trapezoidal cross section having a bottom width of 3.05 feet, as shown in Figure 9.

Wave absorbers and wave filters were placed in the wave channel for the purpose of eliminating, insofar as possible, the undesirable reflected waves. Wave absorbers were placed at the opposite end of the channel from the wave generator, at the transition from

the rectangular to the half-trapezoidal section, and behind the wave generator. The wave absorbers were of the permeable type with impermeable backing, similar to some of the absorbers discussed by Herbich 7/. They consisted of aluminum lathe turnings packed on a sloping plywood panel and covered by wire mesh. Dimensions of the wave absorbers are given in Figure 9, and a photograph of the absorber at the down wave end of the channel is shown in Figure 10. The effectiveness of the wave absorbers was demonstrated by the complete subsidence of wave motion within a very short time after shutting off the wave generator.

Two types of wave filters were used. These were placed as shown in Figures 9 and 10. The parallel plate filter consisted of 26-gage galvanized iron sheets spaced at 2-inch intervals across the channel. This filter was constructed in two sections, each 3 feet in length, placed end to end. Corrugated sheets of perforated metal lath were inserted in the bays between the galvanized plates. The curtain filter was located in the channel a short distance downstream. It consisted of three vinyl plastic sheets cut to the shape of the channel cross section, suspended at the top of the channel, and weighted at the bottom with a length of rod. These curtains, or diaphragms, were placed at right angles to the channel alignment and were spaced at 12 inches. Corrugated sheets of perforated metal lath were tacked to the sloping sidewall between the two filters to suppress the waves from breaking along the sloping sidewall. The filters were required in order to minimize effects of the transverse wave motion which became apparent when the wave generator was first tested without filters. The phenomena associated with the transverse wave motion will be discussed in greater detail in the section dealing with waves in trapezoidal channels.

The parallel plate filter and the corrugated lath tacked to the sloping sidewall performed their functions fairly effectively. However, the effectiveness of the curtain filter remained questionable.

The test section, located about 20 feet down the channel from the filters, measured 8 feet in length and 6 and 1/2 inches in thickness, Figures 9 and 12. The test section was backed by a heavily reinforced 3/4-inch plywood panel. The purpose of the reinforcing was to minimize vibrations during compaction. The backing was covered by perforated metal lath for the purpose of improving the bond between plywood and soil. During the calibration, the test section was covered by a plywood panel set flush with the 1-1/2:1 sloping sidewall of the channel.

Wave generator. The wave generator, Figures 9, 10, and 11, was of the rigid flap type hinged at the channel bed as described by Biesel and Suquet 1/. The expression given for the amplitude of

a wave generated by this type of mechanism is

$$a = 2e \frac{\sinh my (1 - \cosh my + my \cosh my)}{my (\sinh my \cosh my + my)} \quad (4)$$

in which y is the mean water depth, e is the maximum displacement from the vertical of the flap projected along the mean water level, and $m = \frac{2\pi}{L}$, where L is the wave length.

The flap was driven by a connecting rod and crank which were powered by a 3-horsepower, 1,155-revolutions per minute, 440-volt alternating-current motor. The motor speed was geared down through a variable speed pulley device, and a system of chains and sprockets. By means of the variable speed pulley system, frequencies could be varied from 20 to 100 waves per minute.

The radius of the crank, which was connected to a 3-foot-diameter flywheel, could be varied from 4 to 15 inches. For a depth of 1.5 feet, this corresponds to a variation in stroke or displacement e of from 0.11 to 0.41 foot.

The connecting rod length was also adjustable to permit equal flap displacements from either side of the vertical over the whole range of stroke settings.

The flap itself consisted of a double thickness of 3/4-inch plywood reinforced by steel angles and fastened to the bed of the channel by four 1/2-inch brass hinges.

Description and use of measuring equipment. Quantities to be measured included the wave height, frequency, celerity, and length, the mean water depth, the dry unit weight of the compacted earth test embankment, and the volume of earth material eroded from the test section.

Wave heights were determined by a movable point gage with electrical modifications. A light flashed on when the point made contact with the water surface and off when contact was broken. Wave heights could be determined quite accurately by reading the crests and the troughs, and then subtracting the trough elevation from the crest elevation. The point gage readings were referenced to the average bed elevation of the channel. The point gage was mounted

to permit movement either across or along the channel over the length of the test section. The result was, in effect, a three-dimensional coordinate system.

Wave frequencies were determined by counting the number of waves passing a given point in a given time interval, usually about 1 minute. The time interval was measured by a stopwatch.

Wave celerities or velocities were determined by timing the travel of a single wave over a known distance with a stopwatch. In the calibration, a distance of 30 feet was used.

Wave lengths were measured by using two point gages equipped with flashing lights. The distance between the gages along a line parallel to the channel alignment was adjusted until the flashes became synchronized. The point gages would then be a definite number of wave lengths apart. The wave length could then be determined by measuring the distance between the gages and dividing by the number of wave lengths. An alternate method for determining wave lengths was to apply the fundamental relationship

$$L = CT \quad (5)$$

in which L is the wave length, C the wave celerity, and T the wave period which is equal to the reciprocal of the frequency. Wave length determinations by these two methods checked to within 0.1 foot.

The equipment used for measuring wave heights and wave lengths is shown in Figure 11.

The mean water depth was determined by subtracting the average elevation of the channel bed from the elevation of the stillwater surface. The average bed elevation was determined by averaging a number of elevations determined at different points along the bed with an engineer's level and rod. A stationary point gage mounted over the calm water behind the wave absorber at the end of the channel opposite the wave generator permitted making mean water depth readings during tests. The relatively small amounts of water lost by splashing and leakage could thus be replaced during testing.

Dry unit weights or dry densities of the compacted embankment was determined before each test by driving standard 62.4 cc density rings into the embankment, removing and weighing the soil cores, and determining the moisture contents. During the

latter part of the testing program, spot density estimates were also made using a Proctor penetration needle.

The volume of eroded material was determined from cross-sectional measurements made at 1-foot intervals along the test section by means of a movable point gage on which a hinged footplate was mounted. The arrangement is shown on Figure 13, where the footplate can be seen resting on the embankment at the bottom of the point gage staff.

Description and use of compaction equipment. The equipment used for compacting earth into the test section is shown in Figure 13. The earth was compacted in layers roughly parallel to the slope by the action of an air hammer on a 2- by 6-inch plank which rested directly on the embankment. The plank helped to distribute the compactive effort more evenly. Between tests, the earth was passed through a 1/4-inch mesh mechanical rotary sieve in order to break up the clods and permit uniform distribution of moisture throughout the soil prior to compaction.

Calibration of Equipment

The calibration consisted primarily of the selection of, and measuring the properties of the different waves to be used in the erosion tests. Spot measurements for other wave conditions were made to extend the calibration data over a wider range and to check the actual wave characteristics occurring in the wave channel with respect to wave theory.

During the initial testing of the laboratory wave facilities, it soon became apparent that wave motion was too complex to be described in simple two-dimensional terms. The sloping sidewall induced a secondary transverse wave motion, also called an edge-wave system, which was superimposed on the main wave train. The edge-wave system was observed to interfere with the basic wave pattern in varying degrees depending primarily on the length and frequency of the generated wave. For short, high frequency waves, the interference was relatively slight, but for long, low frequency waves, the edge-wave interference increased to such an extent that the basic wave pattern became unrecognizable before reaching the end of the channel. Installation of wave filters helped, to some extent, to improve the stability

of the basic wave pattern. The problem of waves in trapezoidal channels is discussed more fully in a later section.

The problem of selecting the waves to use in the erosion tests thus became more complicated. Not only was it necessary to choose waves representative of those occurring in canals, but barring extensive modifications in the experimental setup, it also became necessary to choose waves which could be reasonably stable in the laboratory channel.

Using these criteria, five waves were selected. The subsequent testing program was built around these waves. It was decided that for the first three waves, the frequency f would be held constant at 60 waves per minute, and the wave height varied by setting the generator crank radius R at 5, 8, and 11 inches. For the fourth and fifth waves, R would be held constant at 5 inches, and f set at 50 and 75 waves per minute, respectively. This scheme would enable study of the effects of both the wave height, independent of frequency, and the frequency, independent of wave height. It was decided to hold the depth constant at 1.50 feet for all five waves.

Calibration procedure. Measurement of wave characteristics was also complicated by the effect of the sloping sidewall. There was a variation in wave height across the channel, and the edge waves along the sloping sidewall tended to be unstable. In addition, there was an apparently cyclical variation of wave height both with respect to distance along the channel and with respect to time at a point. The former was more pronounced, particularly for the edge waves.

In order to obtain the average wave characteristics, a large number of wave measurements were taken in the region of the test section. These were averaged, and the result was defined as the average wave.

Elevations of wave crests and troughs were measured with a point gage with flashing light at nine points across the channel. These measurements were repeated at 1-foot intervals along the 8-foot length of the test section. Wave length measurements

by the synchronous lighted point gage method were made both near the vertical wall and near the sloping sidewall. By placing the two point gages with flashing lights on opposite sides of the channel, the phase difference between the main wave and the edge wave was determined. Wave celerities along the vertical wall were also measured. Wave lengths and celerities were measured as described in a preceding section on description and use of measuring equipment. Wave frequencies were checked at fairly regular intervals, and the variable speed pulley mechanism on the wave generator was adjusted as required. The entire series of measurements was repeated for each of the five waves which had been selected for the subsequent tests.

The calibration data were extended to include a wider range of f and R , and a mean water depth of 1.00 foot. This was done by making spot measurements of wave heights in the test section and measuring the wave celerities, from which wave lengths were computed.

Results and analysis of calibration. The characteristics of the five waves as averaged along the length of the test section are shown in Figure 14. Photographs of the same waves are shown in Figures 18-20. In Figure 14, the edge waves are shown as being one-half wave length out of phase with the main wave. This tendency of the edge wave is evident from the photographs and was also proved by measurements which showed the length of the edge wave to be nearly the same as the length of the main wave, and the phase difference to be almost exactly one-half wave length. These measurements were difficult to make, however, due to unstable nature of the edge waves, particularly for the long, low frequency waves. At a distance Z from the sloping sidewall, there was a node which in actuality was a zone of very slight wave motion.

Measurements of wave heights along the test section showed a variation in height of the main wave along the vertical wall of about plus or minus 5 percent and a variation in height of the edge wave ranging from plus or minus 16 percent for Wave 4 ($L = 3.2$ feet, $f = 75$ waves per minute) to plus or minus 50 percent for Wave 5 ($L = 6.8$ feet, $f = 50$ waves per minute).

In all of the subsequent analysis referring to the laboratory wave tests, wave characteristics are defined as those of the main wave,

as measured along the vertical wall of the test section. This appears reasonable in that the edge-wave characteristics are a direct function of the properties of the main wave.

Figure 15 is a dimensionless wave height plot. The plotted points are seen to fall below the theoretical curve for waves generated by a rigid flap type generator hinged at the channel bed. This is very probably a result of the attenuating effects of the wave filter. It is well known that wave filters cause greater attenuation of short, steep waves than of long, low waves. This is borne out by the position of the plotted points relative to the theoretical curve. It will be noted that the abscissa is a measure of relative wave length.

In Figure 15, and the succeeding calibration plots, Figures 16 and 17, the solid points represent the five principal waves.

Figure 16 is a dimensionless wave celerity plot. The ordinate of the curve on the left C/\sqrt{gy} represents actual wave celerity relative to the celerity of waves in shallow water, and the ordinate of the curve on the right $C/\sqrt{gL/2\pi}$ represents the actual wave celerity relative to the celerity of waves in deep water. The curves are plotted from the equation

$$C = \sqrt{\frac{gL}{2\pi}} \tanh 2\pi y/L \quad (6)$$

which is a transition function of celerities for waves between the deep water and shallow water types. Strictly speaking, Eq. 6 applies only to waves of very small amplitude, however, it approximates celerities for waves of larger amplitude. It is seen from the position of the plotted points along the abscissa that the waves are in the Stokian range, which approaches the conditions for deep water waves.

The wave length plot, Figure 17, shows wave length to be a function of frequency and depth. It is seen that the plotted points, particularly those for $y = 1.50$ feet, do not fall very far from the deep water wave curve. The equation for wave length

$$L = \frac{1.85 \times 10^4}{f^2} \sqrt{\tanh 2\pi y/L} \quad (7)$$

is obtained by combining Equations (5) and (6).

If the frequency, the depth, and the setting of the generator crank are known, the resulting wave length, celerity, and height can be estimated from Figures 15, 16, and 17.

From the calibration, it may be concluded that the laboratory facilities are capable of producing waves varying from approximately 0.10 to 0.50 foot in height, from 3 to 8 feet in length, and from 45 to 80 waves per minute in frequency. Wave heights are limited by the fact that waves become unstable and break as the H/L ratio increases. The breaking index is $H/L = 1/7$ for deep water waves and becomes less when $L/y > 2$. Wave lengths are limited by the breaking index for short waves, and the edge wave interference for long waves.

It may also be concluded that the average characteristics of the main wave are not greatly affected by the edge waves. This conclusion is borne out by the relatively close agreement between the observed characteristics of the main wave and those predicted by two-dimensional wave theory.

Waves in Trapezoidal Channels

The secondary transverse wave motion had not been anticipated and at first was quite baffling. It was thought that the edge waves might have been caused by the abrupt transition from a rectangular to a half-trapezoidal channel section. When various modifications to the transition were tried, and the transverse waves persisted it was concluded that this secondary wave motion was probably a characteristic induced by the sloping sidewall, and therefore typical of wave motion in trapezoidal channels. Ensuing observation served to bear out this thesis.

A search of the literature revealed articles by Hanson ^{6/} and Lamb ^{12/}. On the basis of hydrodynamic theory and mathematical reasoning, they described a phenomenon which they called edge waves. Their description tallies qualitatively with observations made in the wave channel. Following is a brief summary of their discussion.

Edge waves are described as occurring in uniform channels with inclined banks. The amplitude of the edge wave diminishes exponentially as the distance from the bank increases, becoming zero at a distance whose projection on the slope exceeds a wave length. Near the edge, a longitudinal node occurs, and the elevation of the edge wave changes sign. Hanson shows a cross-sectional sketch of a wave which is similar to those shown in Figure 14, in which the crest of the edge wave coincides in time with the trough of the main wave, and the trough of the edge wave coincides with the crest of the main wave.

Lamb described waves occurring in triangular channels with 45° side slopes. As the wave length L decreases, the longitudinal nodes approach the edges, the edge-wave velocity approaches that for deep water waves of length L , and a well defined system of edge waves occur. As L increases, however, the celerity of the edge waves becomes great compared to that predicted by theory for long waves, and transverse oscillations occur which go through a gradual variation of phase along the direction of the channel.

A series of edge-wave demonstrations, Figure 21, were made in the laboratory wave channel using a small, hand-operated generator, Figure 20. The hand generator could be operated either with a piston-type motion or with a rocking motion. The demonstrations showed that for short waves $L/y \leq 2$ a well defined system of uniform edge waves occurred. As L/y was increased, the longitudinal nodes moved further from the edge, the edge waves became less uniform, and transverse oscillations appeared. As L/y was increased still further, the wave along the sloping side broke and moved out ahead of the main wave, setting up a secondary wave front which moved diagonally across the channel and was reflected back from the opposite side.

Motion pictures of wave action in the concrete-lined Delta-Mendota Canal clearly show a well defined system of edge waves occurring along the sloping sides.

The evidence eventually became conclusive that edge waves and the related transverse oscillations are natural characteristics induced by the sloping sidewall, and could therefore not be attributed to the transition from rectangular to half-trapezoidal section in the laboratory wave channel.

Results of edge-wave measurements are shown in Figure 22. The distance from the edge to the longitudinal node \bar{z} is clearly seen to be a function of wave length. The edge-wave steepness \bar{H}_e/\bar{z} is also seen to be a function of the main wave steepness \bar{H}/L . If the height and length of the main wave are known, these curves may be used to predict both the average height of the edge-wave \bar{H}_e and the location of the longitudinal node.

On the basis of the preceding discussion, it is concluded that the range of conditions included by the five waves used for the erosion tests, L/y 2.1 \rightarrow 4.5, corresponds to a state of partially or semi-developed edge waves. The condition described by $L/y = 2.1$ (Wave 4) coincides with a system of almost fully developed edge waves, and

as the L/y ratio becomes greater, the stage of development accordingly becomes less. Furthermore, it seems likely that the edge-wave reflections from the vertical wall of the wave channel are minor when the wave length is less than the channel width at the waterline. Reflections from the vertical wall may become an important factor, however, when the wave length becomes greater than the channel width.

Erosion Tests on Driftwood Canal Soil

The primary object of the erosion tests was to determine the relationship among the variables involved in the erosion of canal banks by wave action. These variables include both wave characteristics and soil properties. A secondary object was to evaluate and, where possible, to improve the test procedure and the test facilities.

Soil Characteristics. The soil used in the erosion tests was taken from locations between Stations 9+80 and 11+00 along the Driftwood Canal near McCook, Nebraska. The Driftwood Canal is part of the Frenchman Unit of the Missouri River Basin Project. The soil is a Nebraska loess, and would be classified in the CL group according to the plasticity chart, Figure 23, of the Unified Soil Classification System. It could also be described as an inorganic silty clay of low plasticity.

Two shipments of soil were received from the field. The first shipment was used in the first erosion test, Run 1-S. The second shipment was received later, and the two shipments were mixed together for the remaining tests.

Various standard properties tests such as those for gradation, specific gravity, Atterberg limits, and compaction were performed on the soil at different times throughout the testing program. The averaged soil properties test results are shown in Figure 24.

The results of the individual tests are tabulated in Tables 2 and 3. Table 4 shows when the soil properties tests were performed with respect to the sequence of erosion tests. There was a relatively minor difference between the properties of the first and second shipments; however, the soil properties apparently were not appreciably affected by the repeated cycles of remolding through which the soil was processed during the test series.

Test procedure. The test procedure was built around the measurement of the erosion rate caused by each of the five waves for which the equipment had been calibrated.

Preparation for a test consisted of breaking up the clods in the soil, bringing the soil to its optimum moisture content, and compacting it into the test section.

The clods were broken up by passing the soil through a mechanical rotary 1/4-inch mesh sieve. The object in breaking up the clods was to permit better distribution of moisture throughout the soil.

The amount of water required to bring the soil to optimum moisture content was determined by weighing the soil, measuring its moisture content by weighing and oven-drying samples, and computing the additional amount of moisture required. Next, the water was added and mixed with the soil. The soil was then covered by wet sacks and a tarpaulin and left for several days during which the moisture distributed itself by capillary movement. An additional mixing after 2 or 3 days helped to speed the process.

When sample moisture determinations indicated that the soil was ready for placement, preparation of the test section was started. The soil was then compacted into the test section with an air hammer. Several methods of using the air hammer were tried. Trial and error experiments indicated the method pictured in Figure 13 to be the most effective. Using this method, the blows of the hammer were transmitted through a 2- by 6-inch plank which was slowly moved over the entire test section. The soil was compacted in layers lying approximately parallel to the 1-1/2:1 embankment slope. The thickness of the layers was usually 1 inch or less.

After the embankment had been built up approximately to grade, it was screeded with a steel straight edge, and the low spots were filled and compacted by hand. Core density samples were then taken along the waterline in order to determine the degree of compaction which had been achieved. Results of these density measurements are shown in Table 5.

Both the compaction technique and the compaction control tended to improve as the test series progressed. A Proctor penetration-resistance needle was used for compaction control purposes when preparing the test section for Runs 4-S and 5-S. A compaction cylinder was prepared according to the specifications of the standard Proctor compaction test immediately before beginning preparation of the test section. Needle readings taken on the cylinder provided a basis for comparison with needle readings obtained in the embankment. This enabled better compaction control.

After patching up the density-core holes and setting the stroke and frequency of the wave generator, the wave channel was immediately filled with water in order to prevent the embankment from drying out. The embankment was allowed to saturate overnight before beginning the erosion test.

In the erosion tests, the wave generator was allowed to run over a measured time interval after which it was stopped. Cross sections of the eroded slope were then taken at 1-foot intervals along the test section. The cross-sectional measurements were obtained by means of a movable point gage with a hinged foot, Figure 13. The wave generator was then started again and run for another time interval after which another set of cross-sectional measurements were taken. The test was thus continued over a number of time intervals until the waves had eroded through the 6 and 1/2-inch thick test section or until the time intervals totaled 12 hours, whichever came first.

The wave frequency was checked by stopwatch at fairly frequent intervals throughout the tests. The variable-speed pulley mechanism was adjusted as required in order to maintain the desired frequency. Frequency adjustments of greater than 2 percent rarely had to be made. The water temperature and depth were checked at less frequent intervals. Water temperatures remained essentially constant, varying from a minimum of 18° C to a maximum of 23° C. Water was added to the wave channel as required in order to replace losses from splashing and leakage. Photographs and motion pictures of the waves and test section were also taken at intervals throughout the tests.

After the test had been completed and the channel drained, the soil was removed from the test section and prepared for another test.

The entire process of preparing the soil, preparing the test section, and performing the erosion test was called a run. The runs were numbered 1-S, 2-S, 3-S, etc. The numbers 1, 2, 3, etc., refer to the numbers assigned to the waves during the calibration. Thus, Run 3-S means the erosion test in which Wave 3 was used.

The amounts of erosion after 12 hours of Runs 4-S and 5-S were relatively slight. Therefore, additional information was obtained by continuing Run 4-S using Wave 3, and continuing Run 5-S using Wave 2. The continuation of Run 4-S was called Run 3-S-A, and that of 5-S, 2-S-A. Run 3-S-B was a continuation of Run 3-S-A and was performed after the test embankment had been dried for 6 days with the help of an electric fan.

Test results. In all of the tests, the initial erosion rate was quite high, but soon diminished with time. The high initial rate was due to the swelling and consequent softening of a thin layer at the surface of the soil which occurred when the wave channel was filled with water. The surface softening was probably due to the fact that the Driftwood soil contains some montmorillonite clay which expanded upon saturation. Slaking may also have been a contributing factor.

The erosion pattern was similar in all tests in that all of the erosion was concentrated near the waterline. After a time, a sloping beach would be formed beneath the waterline. The beach was usually quite stable, and it is probable that the shallow depth of water over the beach helped to dissipate the wave energy, and that this contributed toward a reduced rate of erosion.

In the earlier tests, notably Runs 1-S, 2-S, and 3-S, the compaction in the interior of the embankment had not been as good as the compaction closer to the surface. This was reflected by an increase in the erosion rate after the softer material became exposed to the wave action.

The erosion patterns at the ends of the test section were sometimes not typical of the erosion pattern throughout the rest of the test section. Probable causes for this were reflected waves from the exposed ends of the test section, and a weak bond in the corners of the test section where compaction was more difficult. However, this tendency decreased as the compaction technique was improved.

The erosion cross sections for the middle 6 feet of the test section were averaged and plotted. These plots are shown in Figures 26 through 33. The progression of erosion is shown by the symbolized lines, each one of which corresponds to the average cross-sectional shape at the time specified by the symbol. The time is measured in minutes of wave action from the beginning of the test.

Figures 34 through 39 show several typical photographs taken during and after some of the tests.

Run 3-S-B deserves special mention due to the phenomenal increase in erosion rate which occurred after the embankment had been permitted to dry following Run 3-S-A. The embankment, Figure 37, developed a network of shrinkage cracks and became very hard during drying. Although the soil had remained quite firm during Runs 4-S and 3-S-A, it became soft and mushy as soon as the wave channel was filled with water. The degree of disintegration was roughly proportional to the degree of drying which had taken place, hence, it was especially noticeable near the surface. Figure 37 shows the condition of the embankment after 100 minutes of Run 3-S-B.

The sudden disintegration of the dried soil immediately upon subjection to immersion is attributed to slaking. Slaking is thought to be caused by the sudden release of the capillary tensile forces and the pressure rise due to the compression of the entrapped air which occurs when the soil is suddenly immersed. Capillary tension builds up in the soil during drying and contributes to the shrinkage and cohesion increase which occurs in some soils during drying. The sudden release of capillary tension upon immersion thus causes a corresponding loss of cohesion. Slaking is usually associated with fine-grained soils not having a strong clay binder.

Following Run 2-S-A, four clods were taken from the embankment for the purpose of conducting an elementary wetting-drying, freezing-thawing demonstration. The results of the demonstration are shown in Figure 40. It is seen that the clod which was air dried for a week prior to immersion underwent the most complete disintegration.

Analysis of Results

The results of the erosion tests were analyzed for the purpose of obtaining a better understanding of the relationships among the factors contributing toward the erosion of canal banks by wave action.

Total erosion was plotted against time as a first step in comparing erosion rates for the series of tests. These plots are shown in Figure 41. In these plots and in the following analysis, the erosion \bar{E} is defined as the average volume of soil displaced per linear foot along the middle 6 feet of the test section. A definition sketch of erosion in the test section is shown in Figure 25.

The trend which appears most evident in the erosion versus time plots, Figure 41, is the tendency toward a high initial erosion rate followed by a tapering off. The sudden increase in erosion rate for Run 3-S-B, which was discussed in the previous section, is clearly seen on this plot.

In Figure 42, \bar{E} is plotted against the logarithm of time. The times for Runs 2-S-A, 3-S-A, and 3-S-B were not established from zero, but from the times indicated by transferring the amounts of erosion at the end of Runs 5-S, 4-S, and 3-S-A back to the curves for Runs 2-S and 3-S.

The tendency for the data from each of the runs to plot as a straight line indicates that erosion after starting tends to continue as a geometric progression of time. Runs 1-S, 2-S, and 3-S in their latter stages appear to be exceptions. However, as observed in the previous section, the soil in the interior and close to the ends of

the embankment had not been compacted as well as the soil nearer the surface when the test section was being prepared for Runs 1-S, 2-S, and 3-S. It is believed that had the compaction been uniform and the end effects of the test section eliminated, the erosion would have continued as a geometric progression of time during the latter stages of these runs. The fact that Runs 2-S-A and 3-S-A plot as straight lines supports this conclusion when it is considered that the waves used in Runs 2-S and 3-S had the same characteristics as those used in Runs 2-S-A and 3-S-A.

It was reasoned that the slopes and intercepts of the straight line relationships plotted on Figure 42 should in some way be related to the soil and wave characteristics influencing the rate of erosion. Therefore, the empirical equation

$$\bar{E} = K_1 \log \frac{t}{5} + K_2 \quad (8)$$

was adapted to the data. In this equation, t is the cumulative test time in minutes, K_1 is the slope of the line or more specifically the amount of erosion occurring during one log cycle of time, and K_2 is the intercept at $t = 5$, which is equivalent to the amount of erosion occurring during the first 5 minutes of the test. The units of \bar{E} , K_1 , and K_2 are ft^3/ft , and $t/5$ is dimensionless. The equation is therefore dimensionally correct.

Various wave and soil characteristics were plotted against K_1 and K_2 . The best correlations were found in the relationships plotted in Figure 43. The significance of the K_2 versus \bar{H} plot is that the erosion of the softened soil near the surface, which takes place during roughly the first 5 minutes, is apparently a function of the wave height only. After the initial period, the K_1 versus \bar{H} plot shows that the erosion rate is controlled by both the degree of compaction, or the density of the soil, and the wave height. Apparently, the degree of compaction assumes increasing importance in controlling the erosion rate as the wave height is increased.

The curves of constant compaction in the K_1 versus \bar{H} plot are essentially empirical and must be considered tentative. There are only a few points on the plot, and compaction is a difficult variable to control, both from the standpoint of uniformity and of accurate measurement. However, the tendency for the rate of erosion to be extremely sensitive to the degree of compaction is unmistakably clear. For example, it is seen from the K_1 versus \bar{H} plot that for a particular wave the amount of erosion in an embankment compacted to 97 percent of the Proctor maximum density would be about three times that in an embankment compacted to 99 percent maximum density.

Attempts at correlating erosion with other wave characteristics such as frequency, celerity, wave energy per unit time, and edge wave size were not successful. In this respect, it is observed that the effects of frequency and edge wave size would tend to counteract each other. As the wave frequency is increased, the wave length and consequently the scale of the edge wave becomes smaller.

In Figure 44, the data are plotted according to Equation 8. The correlation is quite good with the exception of the latter stages of Runs 1-S, 2-S, and 3-S. This exception was discussed previously.

Conclusions

The erosion tests lead to certain conclusions. These conclusions should be considered applicable only to low plasticity, inorganic clays, and silts of a type similar to the Driftwood Canal soil, and should not at this time be extended to include other soil types. These conclusions are listed as follows:

- a. When started, the erosion of a homogeneous embankment by a uniform wave train tends to continue as a geometric progression of time.
- b. The rate of erosion is dependent primarily on the wave height and the density to which the soil has been compacted. Compaction above 95 percent of the Proctor maximum density greatly reduces the erosion rate.
- c. Wetting and drying cycles have a deteriorating effect on the resistance of the embankment to erosion due to disruptive effect of slaking on the soil structure which occurs when dried soil is subjected to immersion. Freezing and thawing cycles seem to have a similar, though not as severe an effect.

SUGGESTIONS FOR FUTURE STUDY

- a. The stability characteristics of other soil types should be investigated, both in the laboratory wave channel and in the field. This should lead to a classification of soil types with respect to resistance to erosion by wave action.
- b. The effect of various wave characteristics such as height, frequency, and celerity on the rate of erosion should be studied further. This could best be done in the laboratory wave channel with several uniform granular soils. The stability of granular soils is dependent primarily on grain size. This would in


effect eliminate density as a variable and permit a better evaluation of the erosion potential of the various wave characteristics.

c. The relationship between compaction and erosion resistance requires further explanation. The present study shows that one is to some extent an index of the other, but this contributes little toward a better understanding of the physical relationships involved.

d. Various methods of stabilizing canal banks should be tested in the laboratory wave channel. Gravel covers, treatment with asphalt and portland cement, protective grass covers, and construction of a stepped bank with a flat slope just beneath the water surface are among the bank protection measures which have been suggested. These studies should lead to the development of rational design criteria for bank protection.

e. Additional data on waves in canals caused by wind velocities in excess of 30 miles per hour would be helpful from the standpoint of further evaluating the modified Sverdrup-Munk-Bretschneider analysis.

f. The behavior of waves in trapezoidal channels both in the field and in the laboratory channel should be investigated further. Edge-wave characteristics are apparently a function of bank slope as well as a function of main-wave characteristics. This may have significant implications with respect to bank erosion problems.



APPENDIX

BIBLIOGRAPHY

1. Biesel, F. and Suquet, F., "Laboratory Wave-generating Apparatus," *La Houille Blanche*, Vol 6, No. 2, 1951, pages 147 to 165 (translated by Meir Pilch, SAF Hydraulic Laboratory, University of Minnesota)
2. Bretschneider, C. L., "The Generation and Decay of Wind Waves in Deep Water," *Transactions AGU*, Vol 33, No. 3, June 1952, pages 386 to 392
3. Bretschneider, C. L., "Generation of Wind Waves Over a Shallow Bottom," *Corps of Engineers, Beach Erosion Board*, T. M. No. 51, 1954
4. Bretschneider, C. L., "Revisions in Wave Forecasting: Deep and Shallow Water," *Proceedings of Sixth Conference on Coastal Engineering, Council on Wave Research, University of California*, 1958, pages 30 to 67
5. Gaillard, D. D., "Wave Action in Relation to Hydraulic Structures," *Professional Paper No. 31, Corps of Engineers, U. S. Army, U. S. Government Printing Office, Washington, D. C.*, 1904
6. Hanson, E. T., "The Theory of Ship Waves," *Royal Society of London, Proceedings, Series A, Vol III*, 1926, page 491
7. Herbich, J. B., "Experimental Studies of Wave Filters and Absorbers," *Project Report No. 44, St. Anthony Falls Hydraulic Laboratory, University of Minnesota*, 1956
8. Hirschberg, L., "Wave Action in Relation to the Design of Hydraulic Structures," *M. S. Report, Colorado State University*, 1949
9. Hufft, J. C., "Laboratory Study of Wind Waves in Shallow Water," *Proceedings ASCE, Proceedings Paper 1765*, September 1958
10. Johnson, J. W., "The Characteristics of Wind Waves on Lakes and Bays," *Transactions AGU*, Vol 29, No. 5, October 1948, pages 671 to 681.
11. Johnson, J. W., "Relationships Between Wind and Waves, Abbots Lagoon, California," *Transactions AGU*, Vol 31, No. 3, June 1950, pages 386 to 392

BIBLIOGRAPHY--Continued

12. Lamb, Horace, "Hydrodynamics," Sixth Edition, Cambridge University Press, 1932, pages 446 to 450
13. Molitor, D. A., "Wave Pressures on Sea Walls and Breakwaters," Transactions ASCE, Vol 100, 1935, page 984
14. Saville, T. Jr., "The Effect of Fetch Width on Wave Generation," Corps of Engineers, Beach Erosion Board, T. M. No. 70, 1954
15. Sibul, O., "Laboratory Study of the Generation of Wind Waves in Shallow Water," Corps of Engineers, Beach Erosion Board, T. M. No. 72, 1955
16. Stevenson, T., "Design and Construction of Harbors: A Treatise on Maritime Engineering," Edition 2, Edinburgh, 1874
17. Sverdrup, H. U., and Munk, W. H., "Wind, Sea, and Swell: Theory of Relationships for Forecasting," Publication No. 601, Hydrographic Office, U. S. Navy Department, 1947
18. U. S. Department of Interior, Bureau of Reclamation, "Hydraulic Model Studies to Determine the Required Cover Blanket to Prevent Fine Base Material from Leaching Due to Wave Action--Kennewick Main Canal, Yakima Project, Washington," Hydraulic Laboratory Report No. Hyd-381, June 1954
19. Carlson, E. J., "Gravel Blanket Required to Prevent Wave Erosion", Proceedings ASCE, Journal of the Hydraulics Division, Vol. 85, No. HY 5, May 1959

LIST OF SYMBOLS

<u>Symbol</u>	<u>Dimensions</u>	<u>Definition</u>
C	L/T	Wave celerity
E	L ²	Average volumetric displacement per foot in middle 6 feet of test section
e	L	Maximum horizontal displacement from vertical position of generator flap, measured at water surface
F	L	Fetch, or length of reach of water over which the wind blows
Fe	L	Effective fetch
f	T ⁻¹	Wave frequency
g	L/T ²	Acceleration of gravity
H	L	Wave height, measured from trough to crest
H̄	L	Average wave height along test section
H _e	L	Average height of edge waves along test section
H _s	L	Significant wave height or average height of 1/3 highest waves
K ₁	L ²	Empirical constant governing rate of erosion. Dependent upon degree of compaction and wave height
K ₂	L ²	Empirical constant dependent on wave height. Equal to amount of erosion occurring during first 5 minutes of test
L	L	Wave length
m	L ⁻¹	$2\pi/L$

LIST OF SYMBOLS--Continued

<u>Symbol</u>	<u>Dimensions</u>	<u>Definition</u>
R	L	Radius of wave-generator crank arm
T	T	Wave period
Ts	T	Significant wave period or average period of highest 1/3 waves
t	T	Cumulative time of wave action measured from beginning of test
t _w	T	Wind duration required to develop waves of maximum size
U	L/T	Wind velocity
U _e	L/T	Effective wind velocity = $U \cos \theta \pm V$
V	L/T	Average flow velocity in canal
W	L	Width of canal at water surface
y	L	Depth of water
\bar{z}	L	Average distance from sloping sidewall to edge wave node projected along stillwater surface line
γ_d	F/L ³	Dry unit weight of earth material
θ		Wind angle, defined as angle between wind direction and canal bearing

Table 1

SUMMARY OF BUREAU OF RECLAMATION CANAL DATA

Project and canal or lateral	Station	Fetch feet	Wind angle	Depth feet	Top width feet	Effective fetch feet	Wind velocity mph	Canal velocity ft/sec	Significant wave height feet	Significant wave per second	L/Y approx.
Eden											
W. Side Lat	57+30	1,200	174°	3.2	27	112	14.2	1.0	0.075	1.25	2.3
Eden	679+00	2,000	137°	3.5	28	136	21.8	2.6	.072	1.70	3.3
W. Side Lat	189+00	500	153°	3.0	26	81	19.6	1.0	.094	0.97	1.8
W. Side Lat	221+00	2,200	123°	3.0	26	133	18.6	1.0	.123	0.97	2.8
Eden Lat	665+84	600	153°	3.5	28	91	20.8	2.6	.094	0.78	1.8
Tucumcari											
Hudson	21+15	1,100	20°	6.0	34	126	16.0	1.3	.070	0.75	1.3
Hudson	385+50	1,100	135°	5.0	31	119	18.0	1.1	.170	1.14	1.3
Conchas	MP56	600	45°	8.2	57	145	18.5	2.1	.080	0.75	1.0
Conchas	MP60.3	800	170°	4.9	29	103	17.5	2.1	.070	1.19	1.4
Central Valley											
Delta-Mendota	MP94.27	4,200	30°	14.0	90	380	15	3.5	.10	1.6	0.9
Delta-Mendota	MP 4.98	98	90°	16.6	98	98	30	3.8	.40	2.5	1.9
Delta-Mendota	MP 4.98	98	90°	16.6	98	98	30	3.8	.20	2.5	1.9
Imperial I. D.											
All-American	4045+00	16,000	175°	11	94	609	30	3.0	.53	2.6	3.1
All-American	4045+00	16,000	175°	11	94	609	30	3.0	.54	2.5	2.9
All-American	4132+90	7,200	175°	12	96	475	22	3.0	.34	3.0	3.8
All-American	4045+00	23,700	30°	11	94	695	21	3.0	.24	1.9	1.7
All-American	3130+00	1,900	138°	13	146	402	28	3.3	.36	2.3	2.0
All-American	3130+00	1,900	138°	13	146	402	28	3.3	.31	2.0	1.6
All-American	3130+00	1,900	153°	13	146	402	16	3.3	.25	1.7	1.2
All-American	3130+00	1,900	153°	13	146	402	16	3.3	.26	2.0	1.6
All-American	3130+00	1,900	153°	13	146	402	16	3.3	.22	2.0	1.6
All-American	4132+90	7,200	175°	12	96	475	18	3.0	.64	2.4	2.5

Table 2

RESULTS OF GRADATION ANALYSES

<div> <div>Sample No.</div> <div>Particle dia in mm</div> </div>	Percent finer than					
	18F-979	18F-1031	18F-1031X	18F-1031X-1	18F-1031X-2	Average
1.190	100.0	100.0	100.0	100.0	100.0	100.0
0.590	99.8	100.0	100.0	99.8	99.8	99.9
0.297	99.7	100.0	100.0	99.4	99.6	99.7
0.149	99.6	99.7	99.6	99.2	99.4	99.5
0.074	97.5	98.8	99.4	97.2	98.0	98.2
0.037	65.8	69.2	68.8	68.8	68.0	68.1
0.019	32.8	37.2	36.8	35.8	37.0	36.1
0.009	17.8	21.2	22.8	23.8	23.0	21.7
0.005	14.4	18.2	16.2	19.8	19.4	17.6

Table 3

RESULTS OF STANDARD PROPERTIES TESTS

Sample No.	LL percent	PI percent	Maximum γ_d pound/foot ³	Optimum moisture content percent	Penetration resistance pounds per square inch	Specific gravity
18F-979	28.2	6.7	104.0	17.8	1,050	
18F-1031	32.0	10.8	106.8	17.2	1,350	2.658
18F-1031X	31.2	10.5	105.3	18.0	920	2.660
18F-1031X-1	30.0	8.8				
18F-1031X-2	29.4	9.2				
Average	30.2	9.2	105.4	17.7	1,110	2.66

Table 4

SOIL SAMPLE DESIGNATION

Sample No.	Place in sequence of erosion tests
18F-979	First shipment of soil. Soil properties determined after receiving from field and before Run 1-S
18F-1031	Second shipment of soil. After receiving from field
18F-1031X	Mixture of both shipments. Soil properties determined before Run 2-S
18F-1031X-1	Mixture of both shipments. Soil properties determined after Run 3-S
18F-1031X-2	Mixture of both shipments. Soil properties determined after Run 4-S

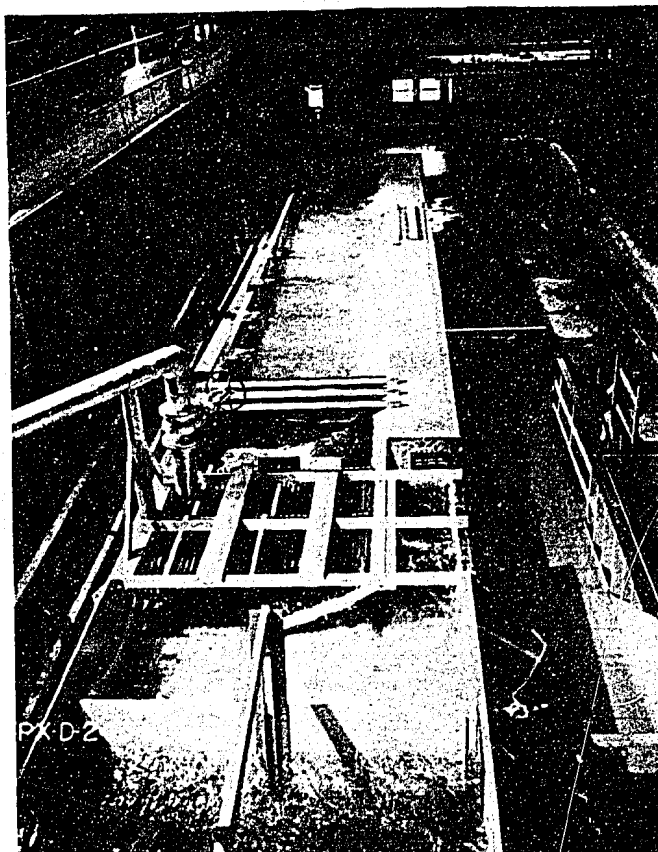
Table 5

RESULTS OF DENSITY MEASUREMENTS

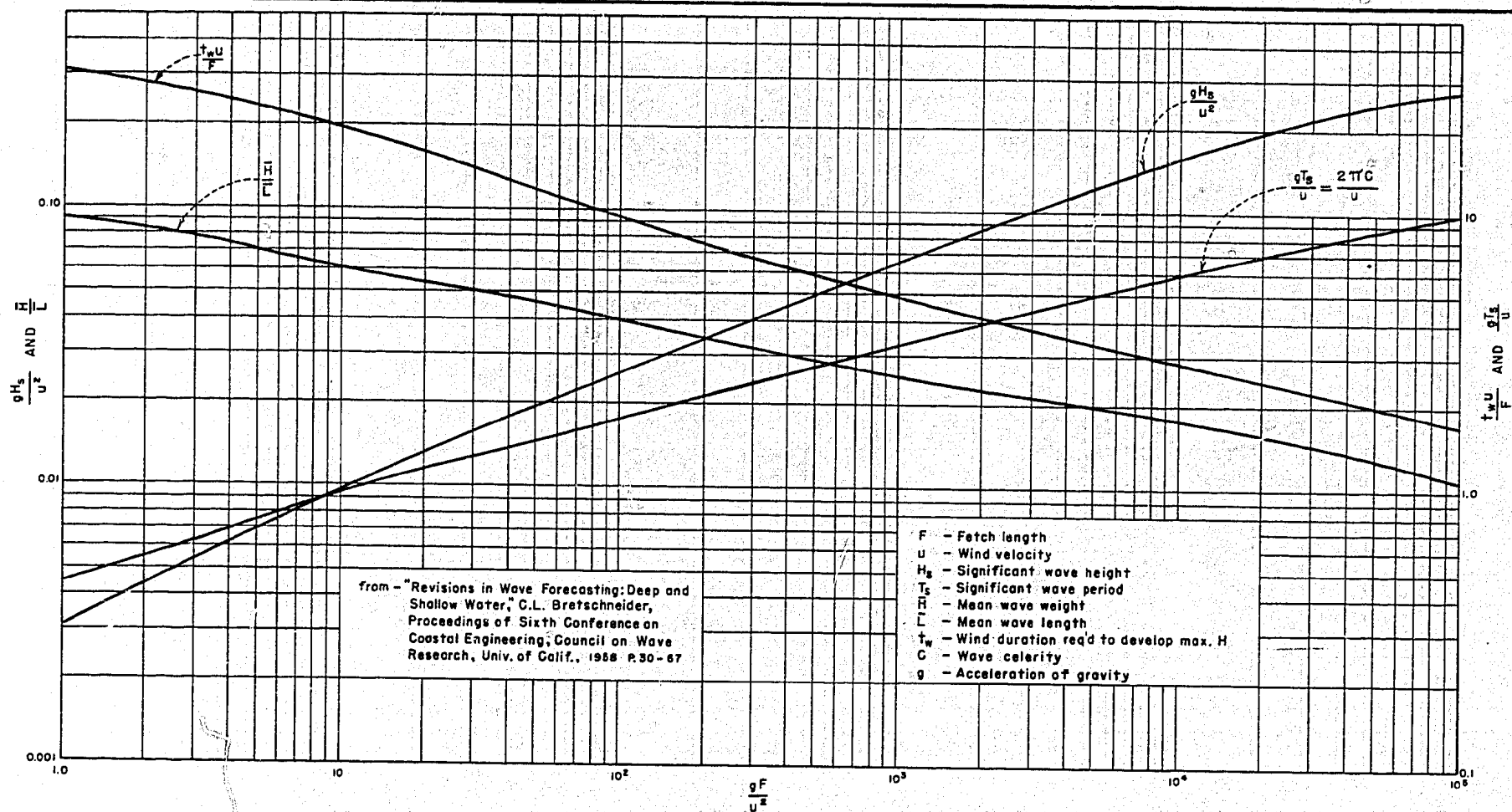
Run	Location of sample		Moisture content percent by weight	Dry unit weight pound/foot ³	Percent maximum dry unit weight
	Station feet	El above channel bed feet			
1-S	0.5	1.5	17.5	101.3	96.1
	2.5	1.1	18.7	100.4	95.2
	5.5	1.1	18.3	104.7	99.2
	7.5	1.5	17.8	103.1	97.9
Average	--	--	18.1	102.4	97.1
2-S	0.5	1.5	17.0	100.4	95.3
	2.5	1.5	17.6	98.5	93.5
	5.5	1.5	17.3	105.5	100.1
	7.5	1.5	17.3	102.6	97.3
Average	--	--	17.3	101.8	96.5
3-S	0.5	1.5	16.6	105.5	100.1
	2.5	1.5	17.6	102.1	96.8
	5.5	1.5	17.3	100.7	95.4
	7.5	1.5	17.1	102.6	97.3
Average	--	--	17.2	102.7	97.3
4-S	0.5	1.5	16.1	105.8	100.2
	2.5	1.5	15.9	105.5	100.1
	5.5	1.5	16.2	105.2	99.8
	7.5	1.5	16.5	103.0	97.6
Average	--	--	16.2	104.9	99.4
5-S	0.5	1.5	17.3	106.2	100.8
	2.5	1.5	17.5	105.3	99.9
	5.5	1.5	17.9	105.6	100.2
	7.5	1.5	16.8	106.1	100.7
Average	--	--	17.4	105.8	100.3



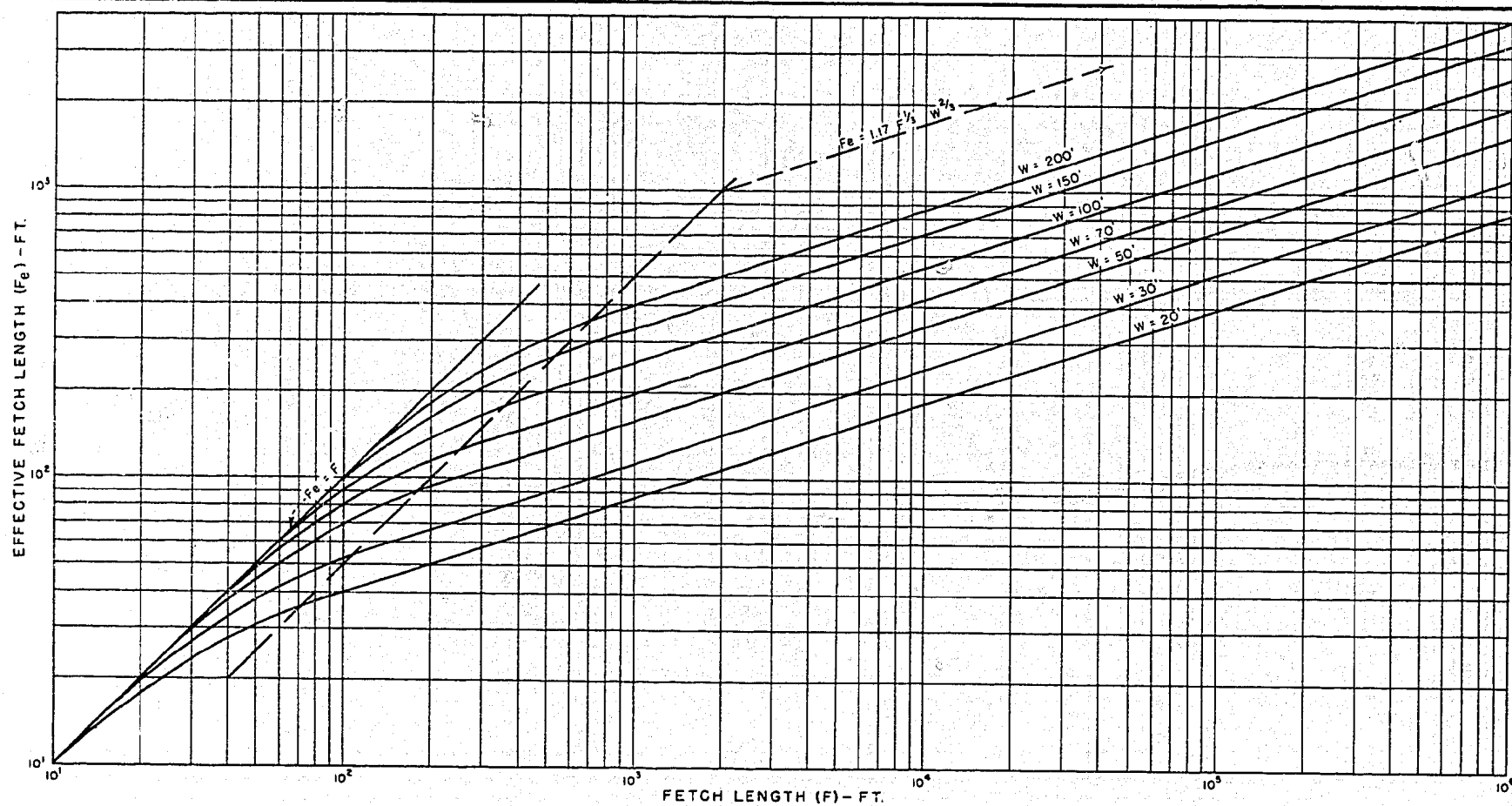
**Wave erosion in Eden
canal after 2 seasons
of operation**



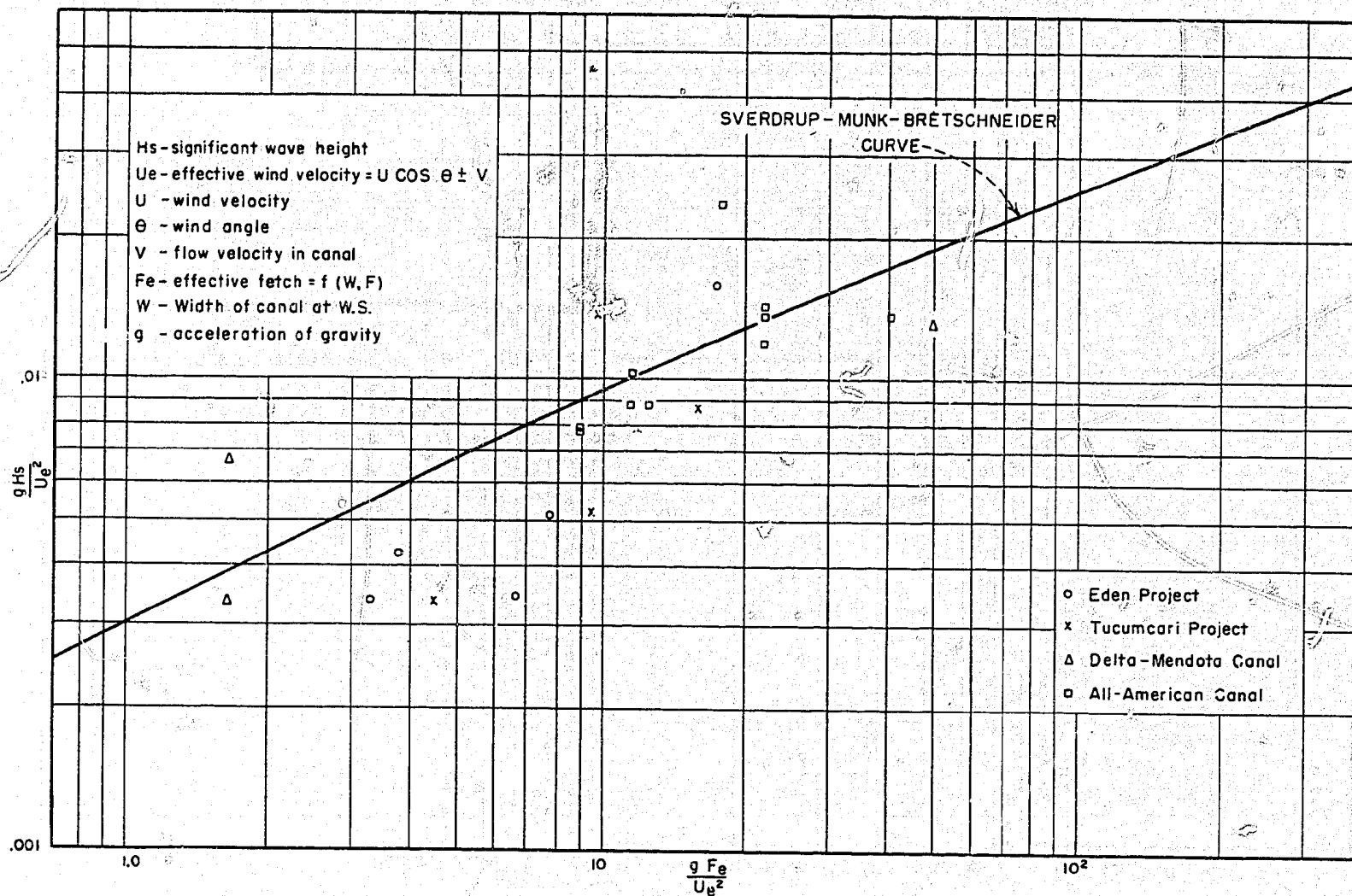
Laboratory wave channel



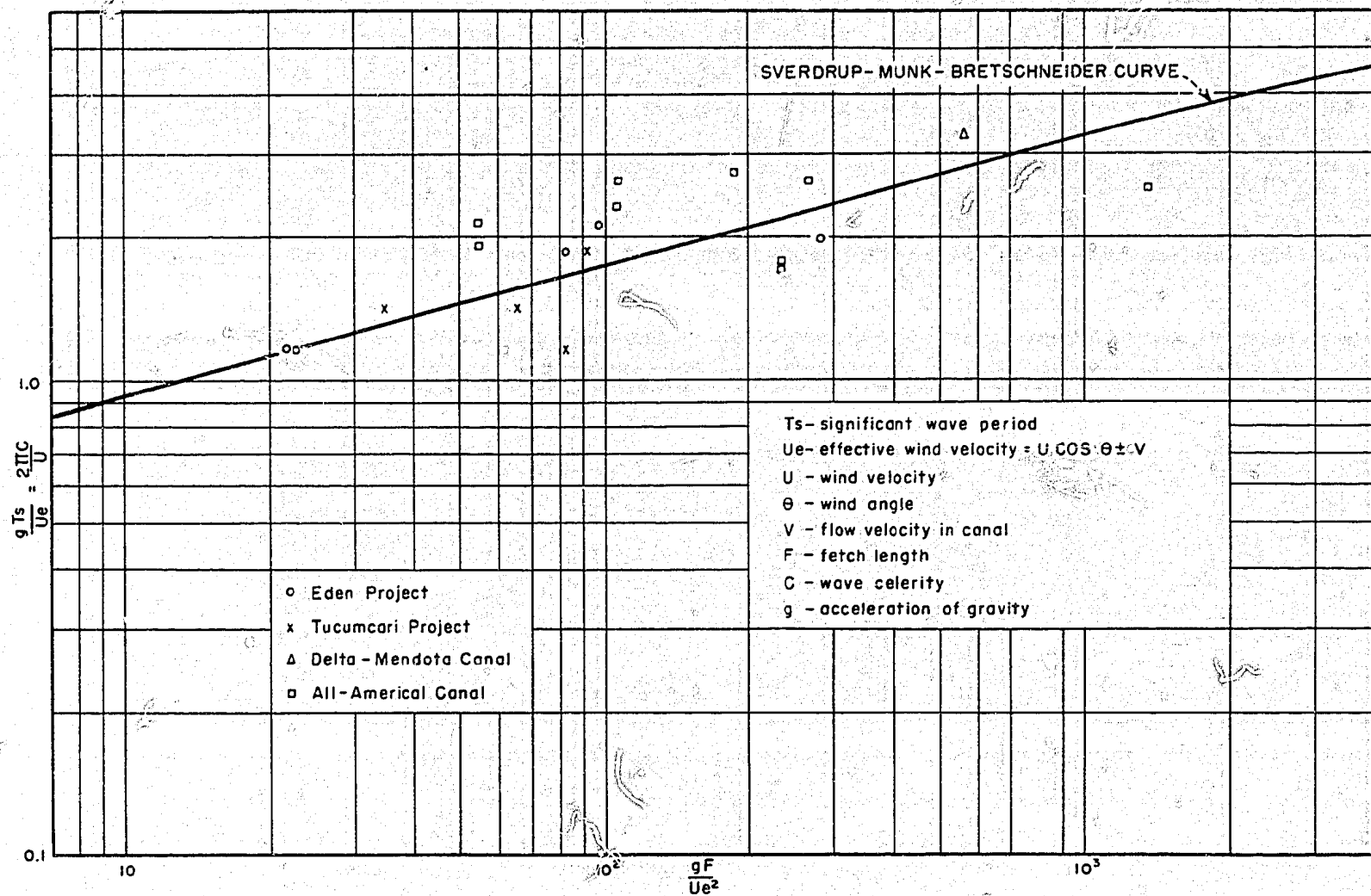
DIMENSIONLESS GRAPH SHOWING RELATIONSHIPS AMONG FETCH, WIND VELOCITY, WAVE HEIGHT, WAVE PERIOD, WAVE STEEPNESS AND WIND DURATION IN DEEP WATER



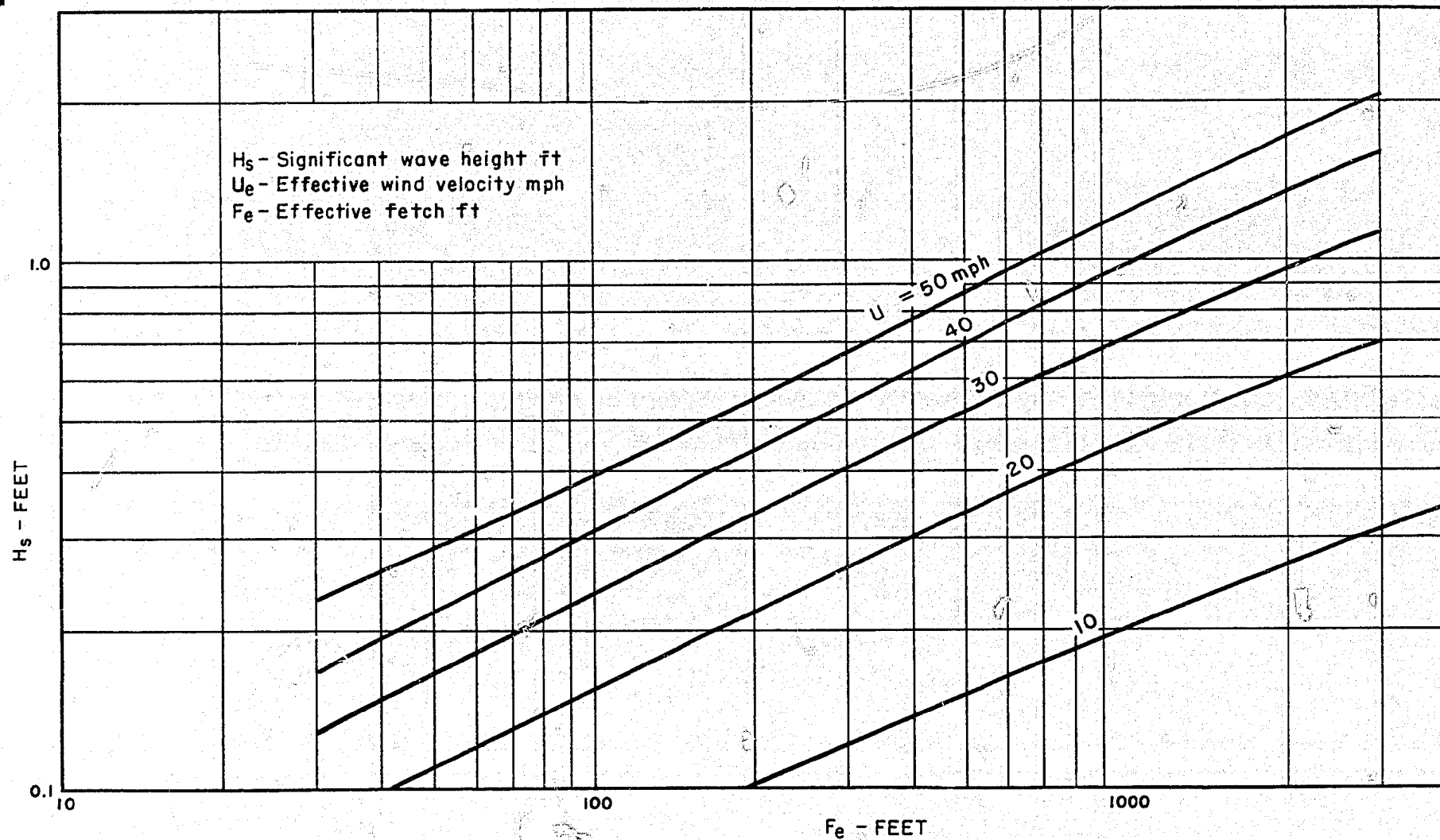
EFFECTIVE FETCH LENGTH AS A FUNCTION OF FETCH LENGTH
AND FETCH WIDTH FOR RECTANGULAR FETCHES
(Data from Beach Erosion Board T.M. No. 70)



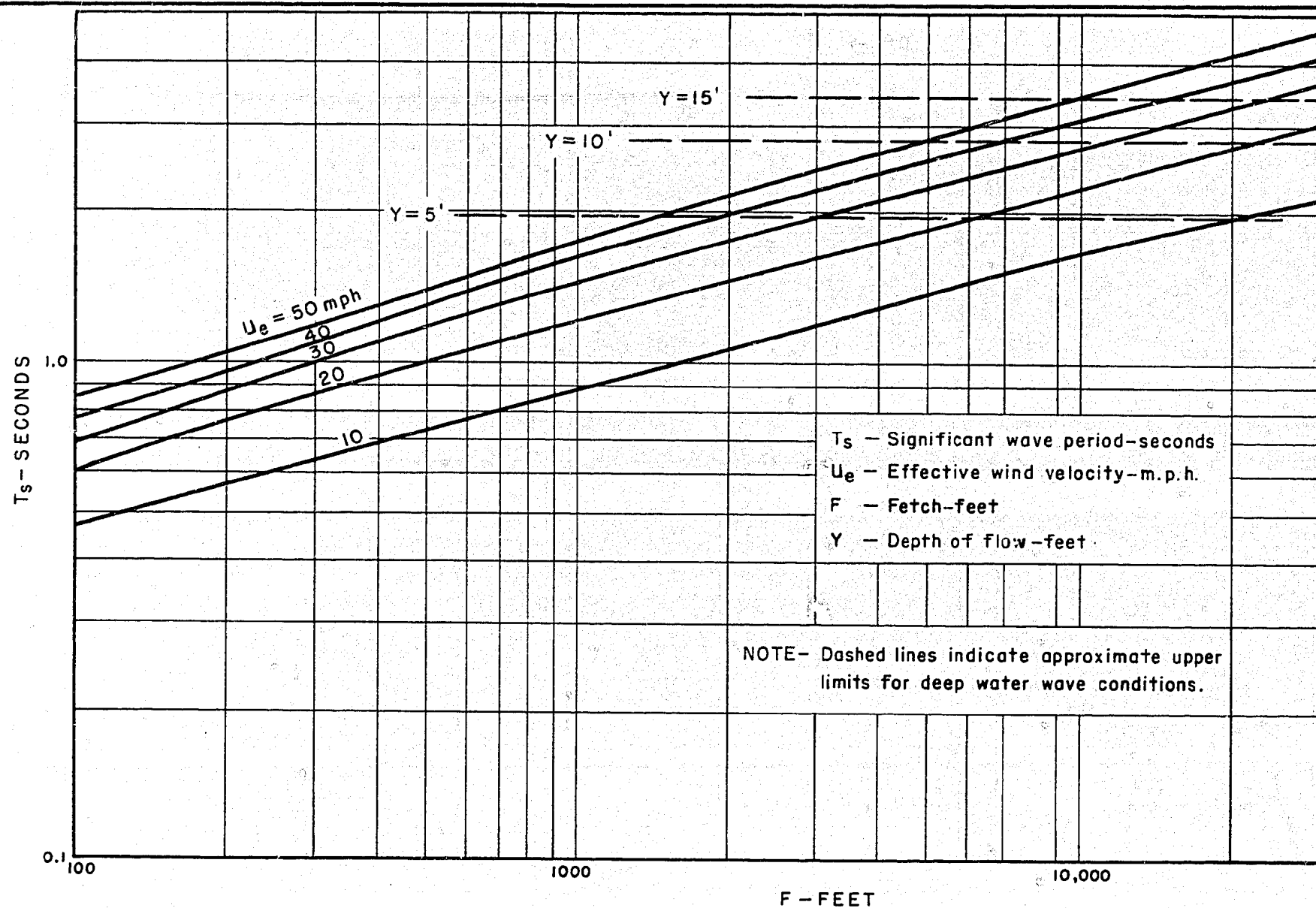
DIMENSIONLESS GRAPH OF WAVE HEIGHT AS
A FUNCTION OF WIND VELOCITY AND FETCH



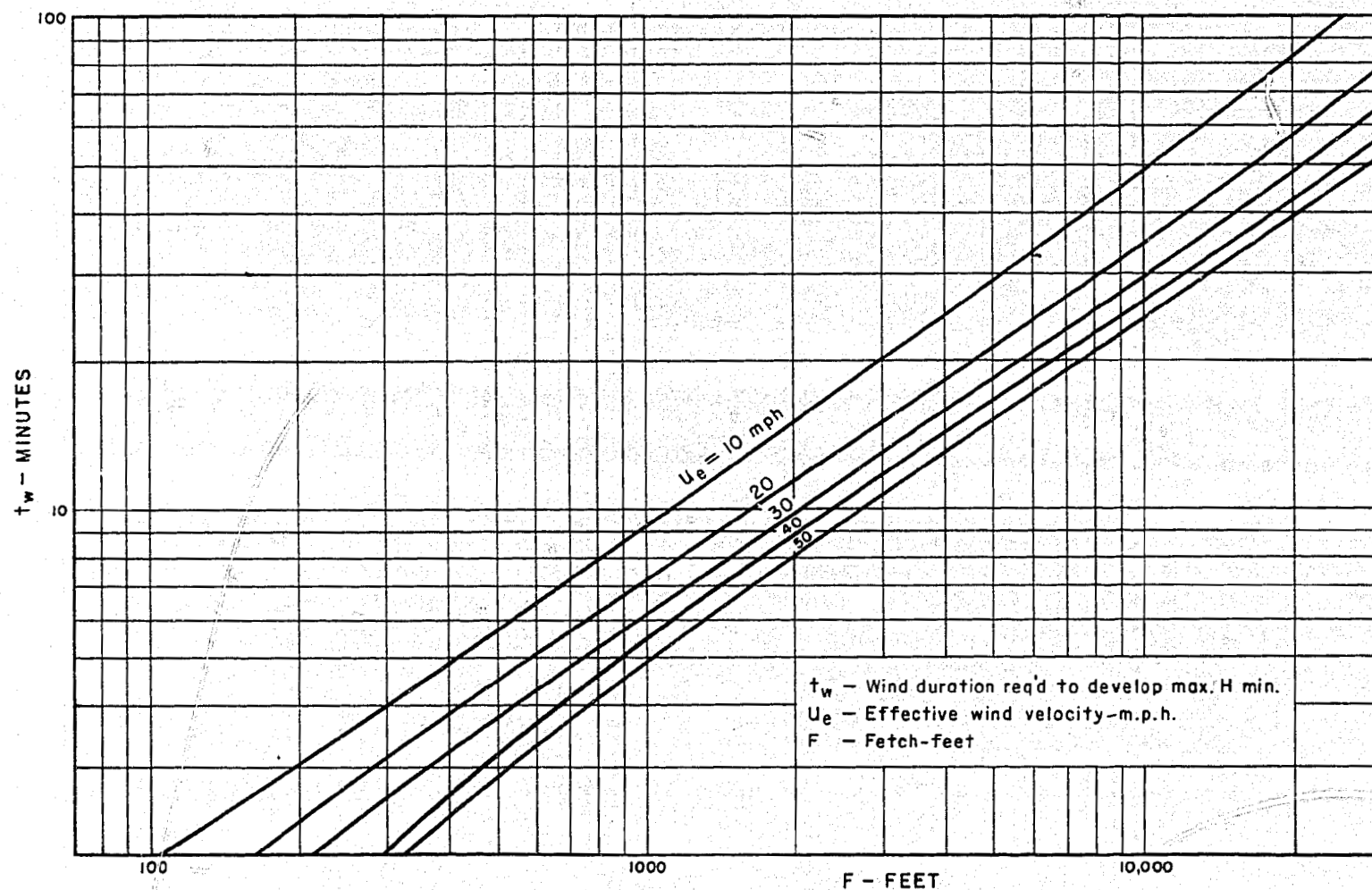
DIMENSIONLESS GRAPH OF WAVE PERIOD AS
A FUNCTION OF WIND VELOCITY AND FETCH



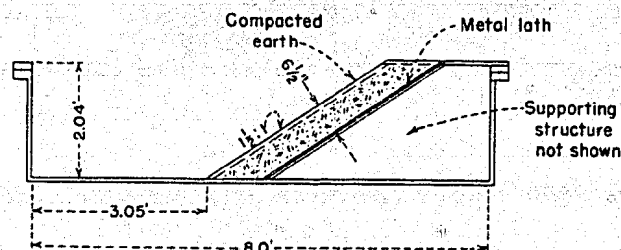
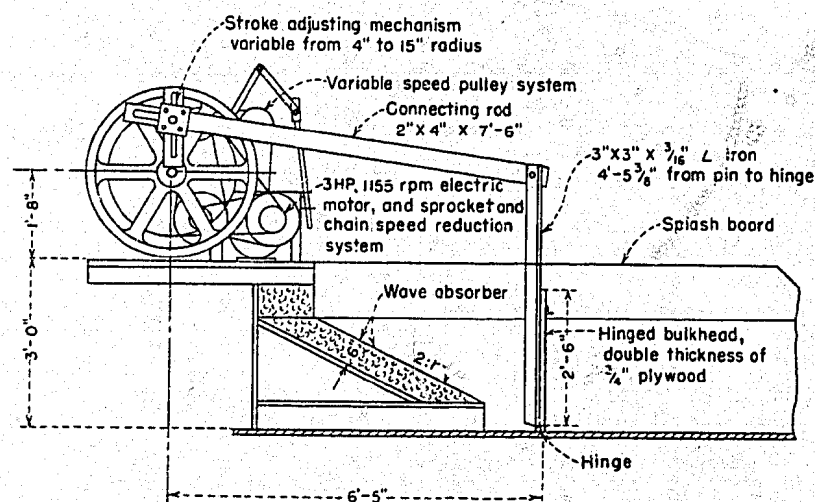
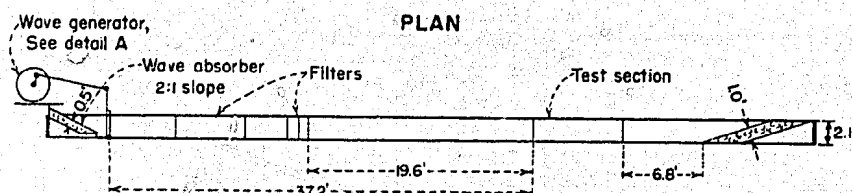
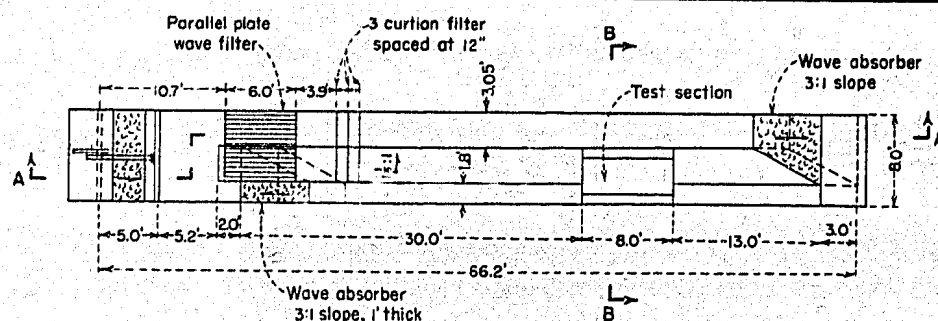
DEEP WATER SIGNIFICANT WAVE HEIGHT AS A FUNCTION
OF EFFECTIVE FETCH AND WIND VELOCITY



DEEP WATER SIGNIFICANT WAVE PERIOD AS
A FUNCTION OF FETCH AND WIND VELOCITY



TIME REQUIRED TO GENERATE MAXIMUM SIGNIFICANT WAVE IN DEEP WATER
AS A FUNCTION OF FETCH AND WIND VELOCITY



LABORATORY WAVE CHANNEL AND EQUIPMENT-SCHEMATIC SKETCHES

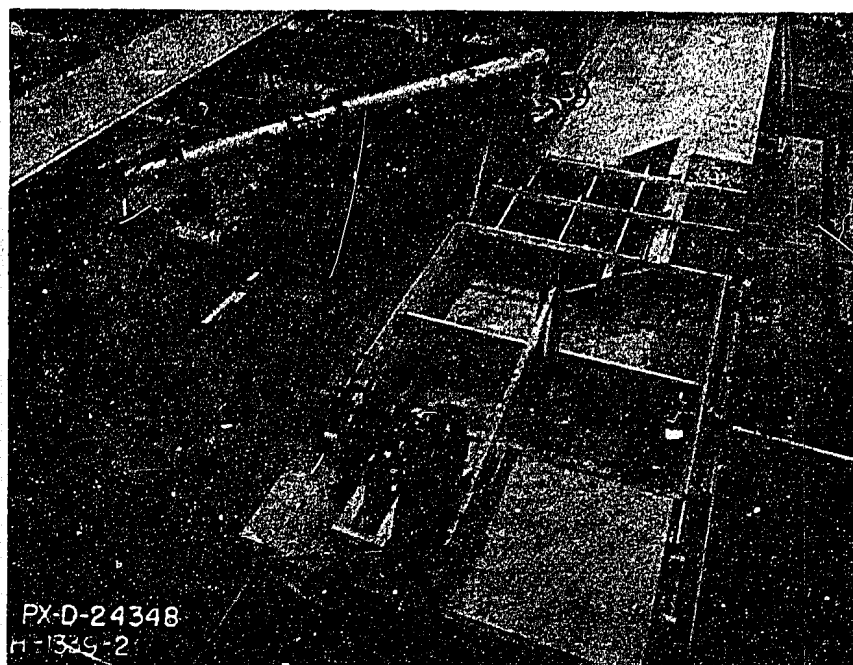


Wave generator
and wave filters

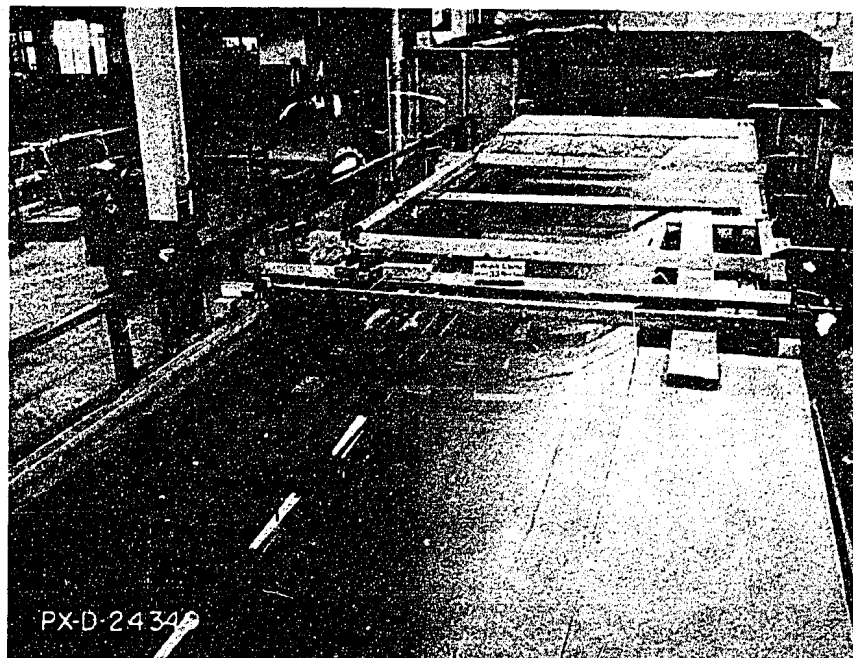


Absorber at
down-wave end
of channel

LABORATORY EQUIPMENT



Wave generator



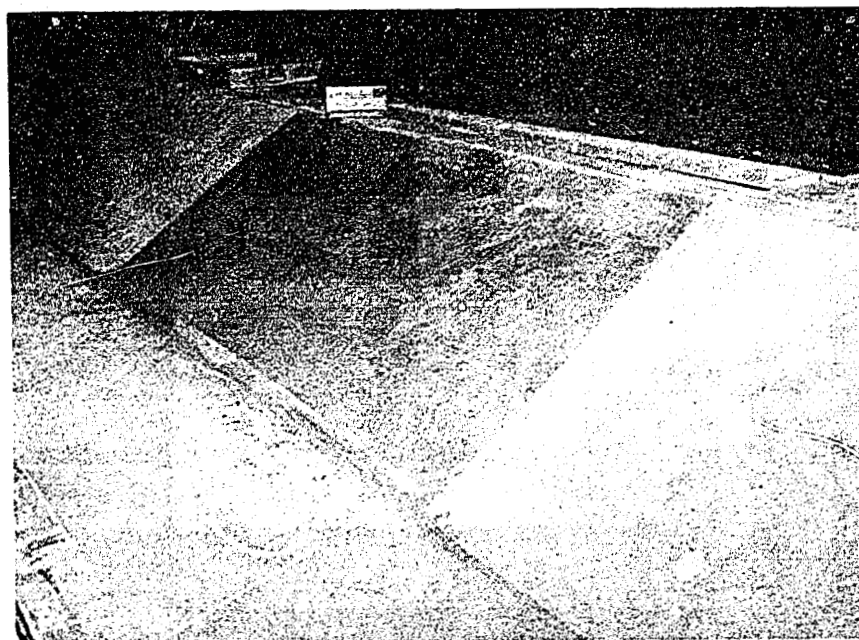
Equipment arrangement
for measuring wave
heights and lengths

LABORATORY EQUIPMENT

FIGURE 12
Report Hyd 465



Empty test section

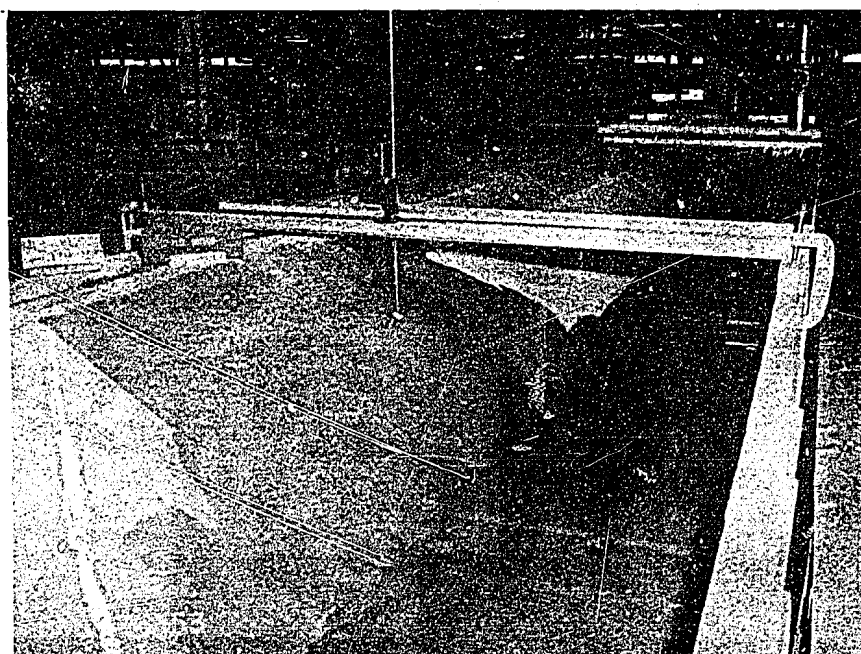


**After compacting
earth into test section**

LABORATORY EQUIPMENT

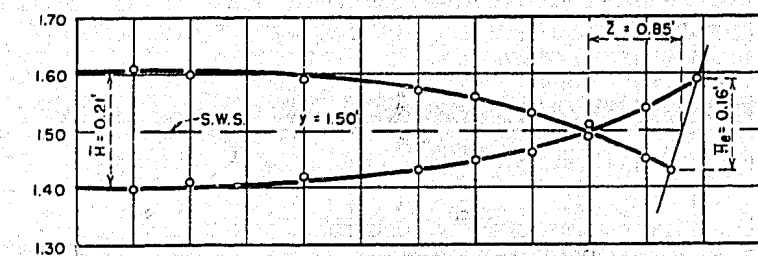


Compaction equipment

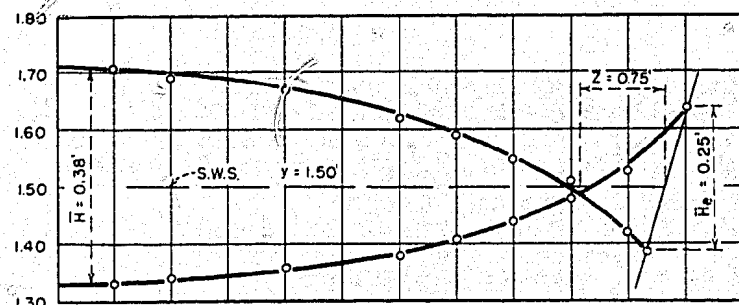


**Equipment for measuring
erosion cross sections**

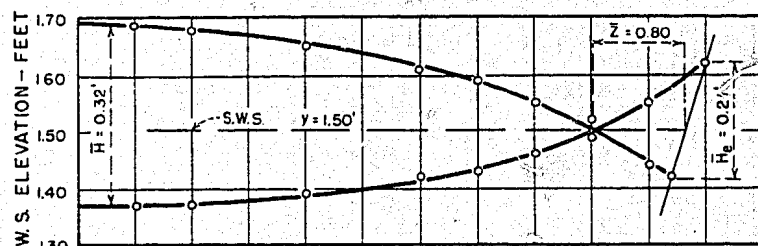
LABORATORY EQUIPMENT



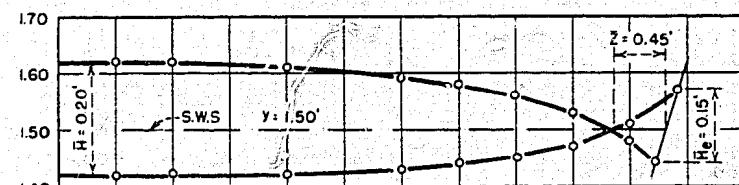
WAVE 1 - $T = 1.00$ SEC., $L = 4.8'$, $R = 5''$



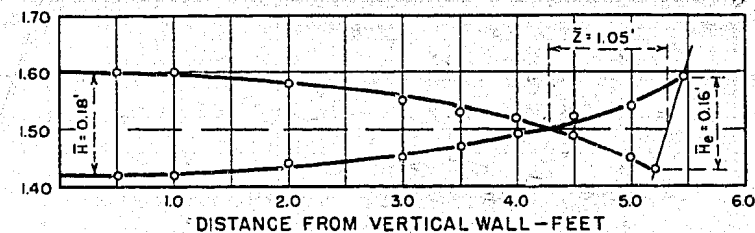
WAVE 2 - $T = 1.00$ SEC., $L = 4.7'$, $R = 11''$



WAVE 3 - $T = 1.00$ SEC., $L = 4.8'$, $R = 8''$



WAVE 4 - $T = 0.80$ SEC., $L = 3.2'$, $R = 5''$



WAVE 5 - $T = 1.20$ SEC., $L = 6.8'$, $R = 5''$

CHARACTERISTICS OF AVERAGE WAVES

SYMBOL	y	R
●	1.50'	.417
▲	↓	.917
■	↓	.667
△	↓	.917
□	↓	.667
x	1.00'	.917
○	↓	.667

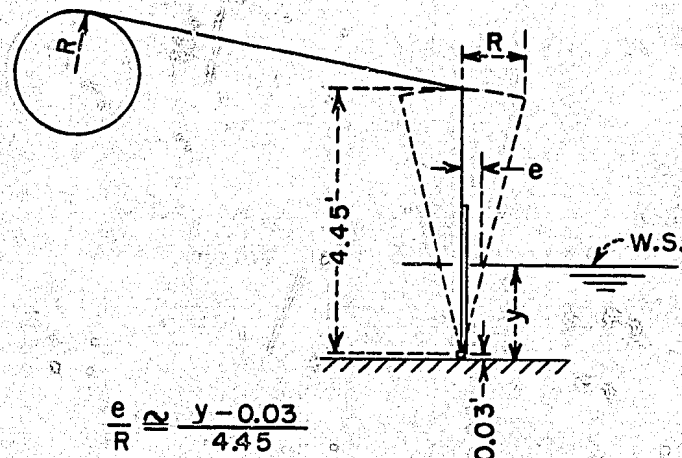
H = Wave height - feet

R = Radius of crank - feet

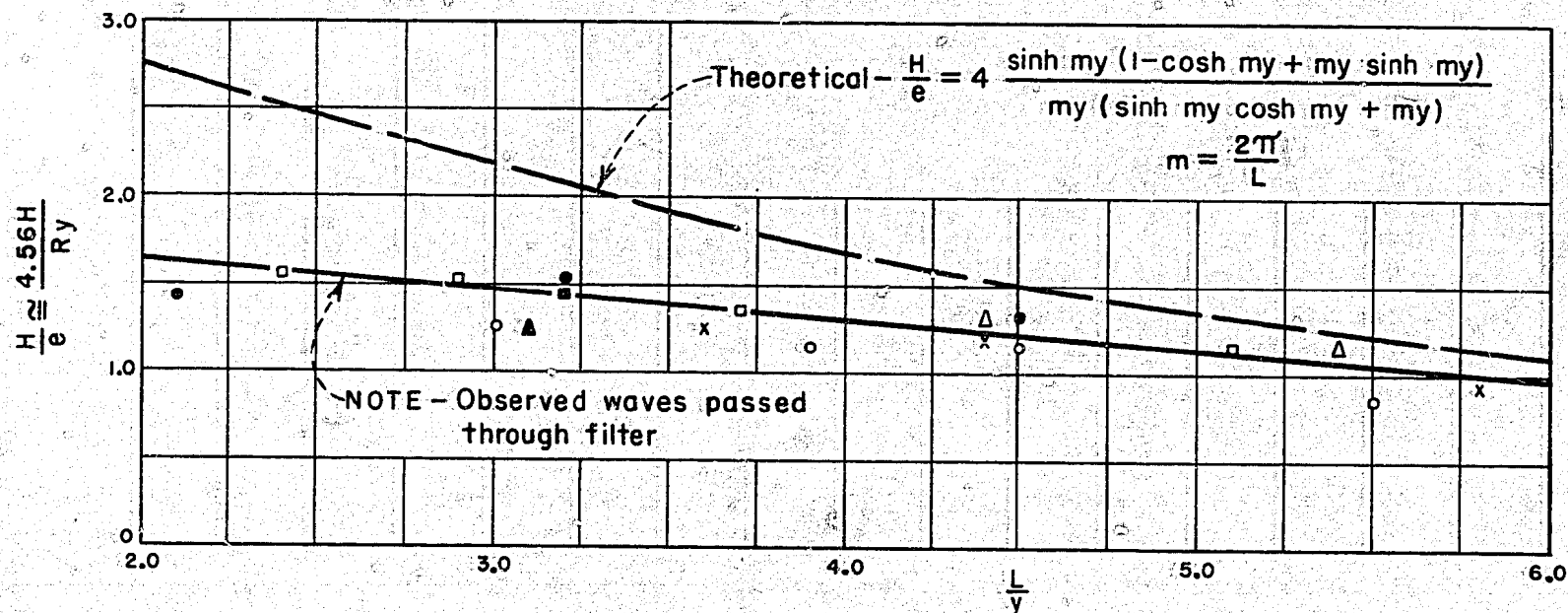
y = Depth of water - feet

e = Displacement of generator
flap at W.S. - feet

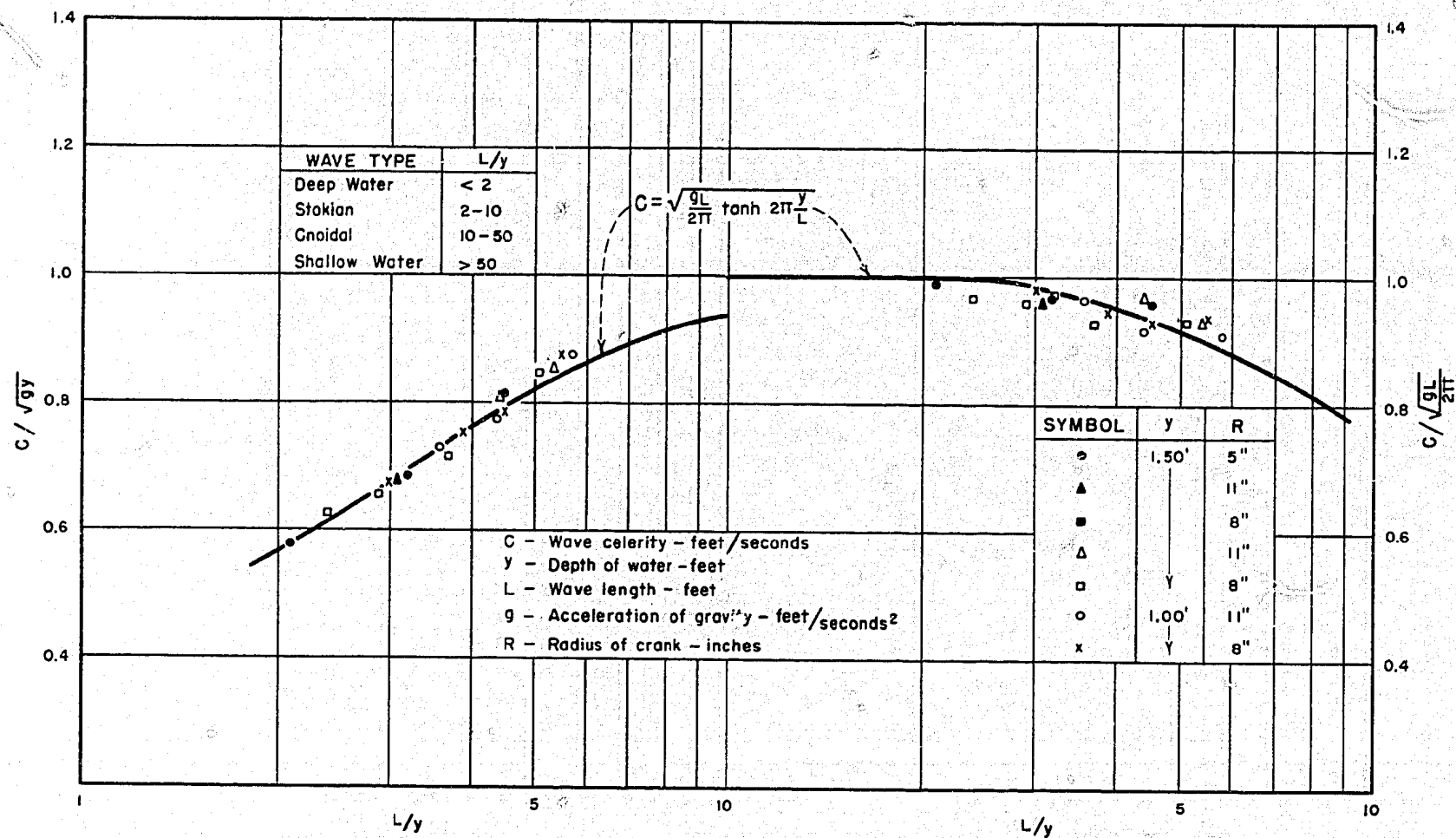
L = Wave length - feet



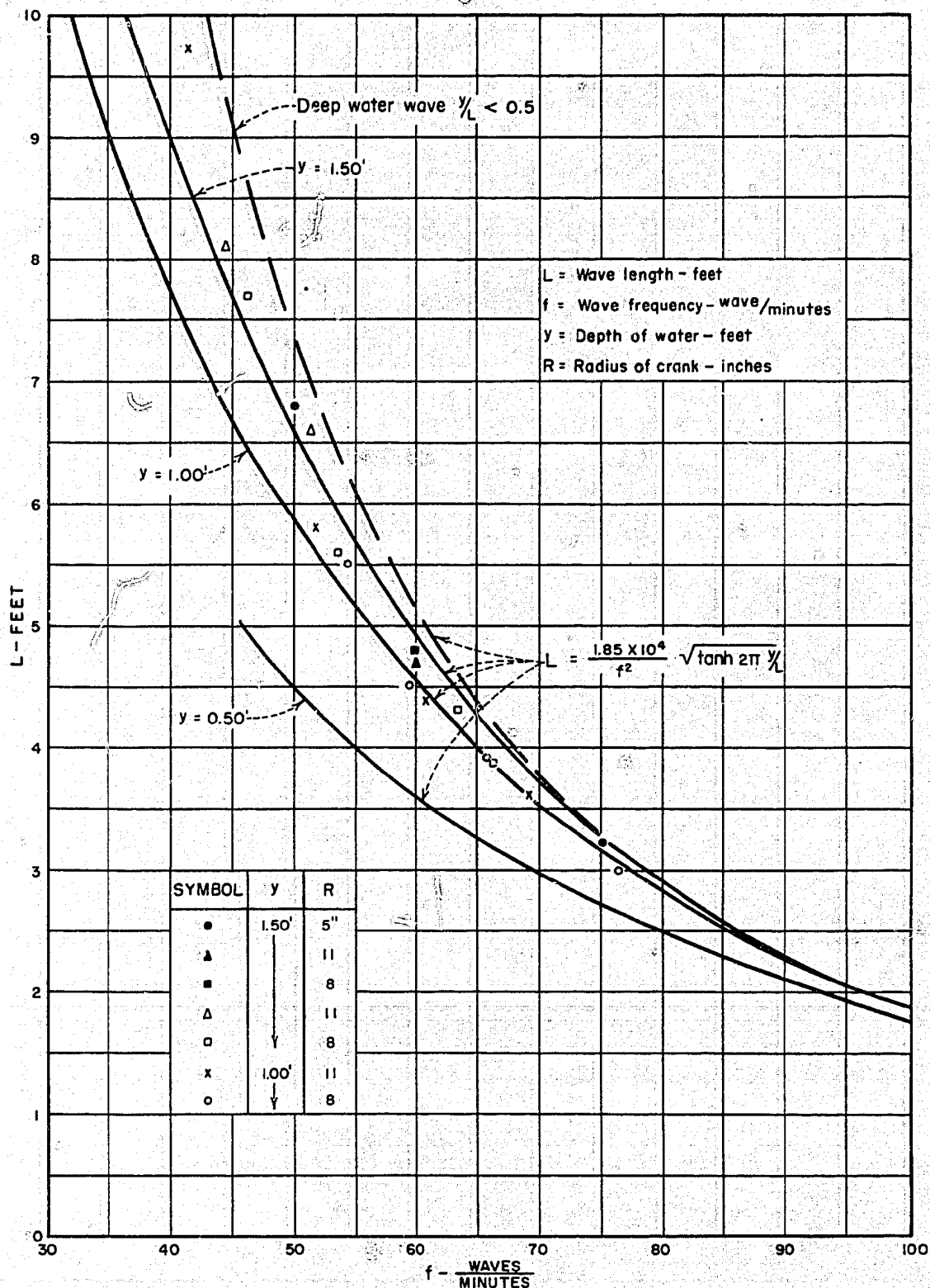
$$\frac{e}{R} \approx \frac{y - 0.03}{4.45}$$



COMPARISON OF OBSERVED WITH
THEORETICAL WAVE HEIGHTS



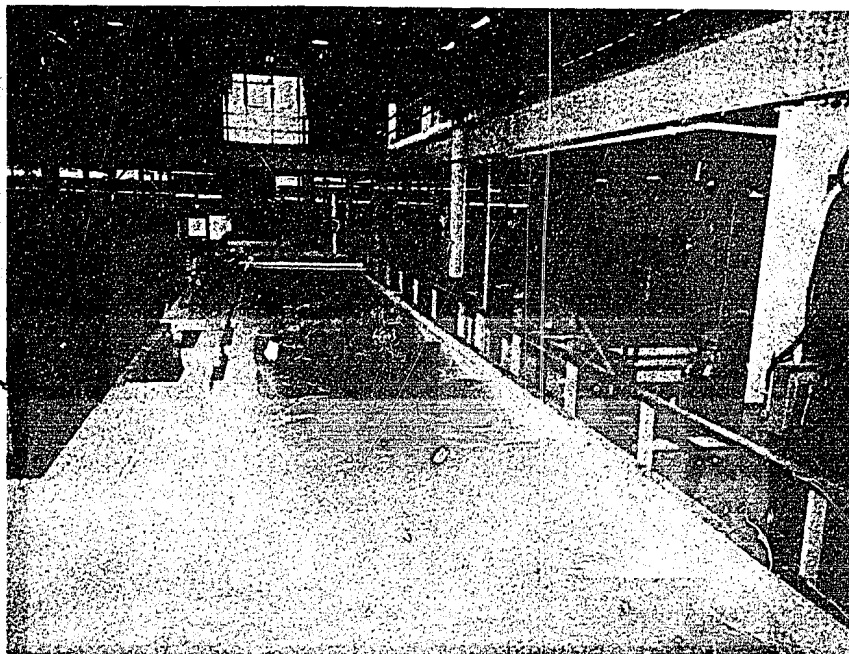
COMPARISON OF OBSERVED WITH
THEORETICAL WAVE CELERITIES



COMPARISON OF OBSERVED WITH
THEORETICAL WAVE LENGTHS



Wave 1 -
 $\bar{H} = 0.21'$
 $T = 1.0 \text{ sec}$
 $L = 4.8'$
 $R = 5''$



Wave 2 -
 $\bar{H} = 0.38'$
 $T = 1.0 \text{ sec}$
 $L = 4.7'$
 $R = 11''$

WAVES USED IN EROSION TESTS

FIGURE 19
Report Hyd 465

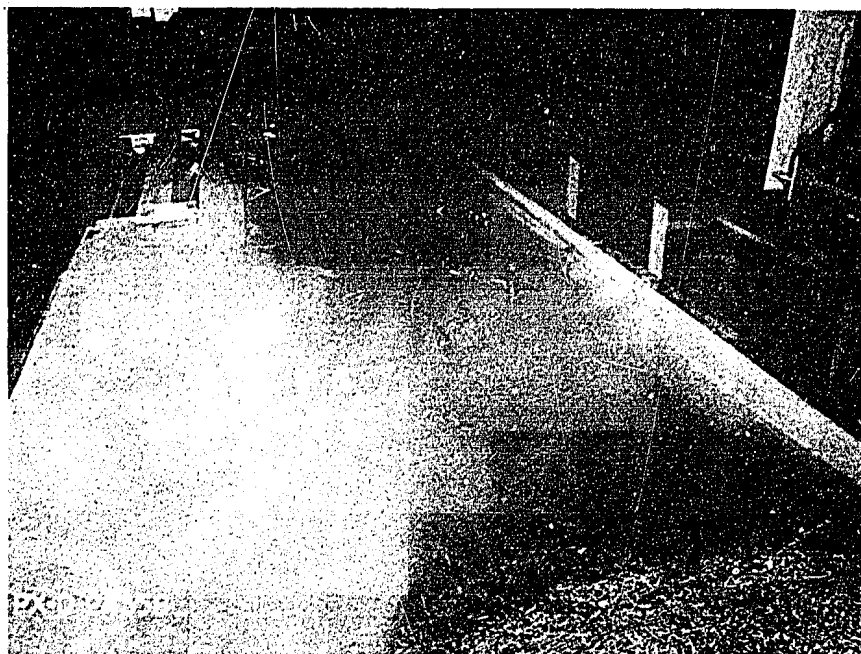


Wave 3 -
 $\bar{H} = 0.32'$
 $T = 1.0 \text{ sec}$
 $L = 4.8'$
 $R = 8''$

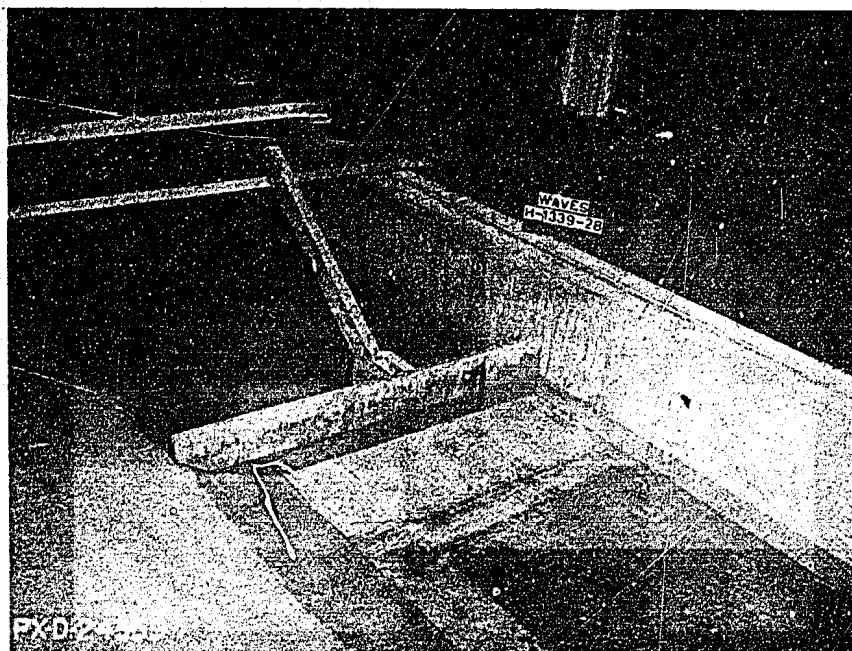


Wave 4 -
 $\bar{H} = 0.20'$
 $T = 0.80 \text{ sec}$
 $L = 3.2'$
 $R = 5''$

WAVES USED IN EROSION TESTS



Wave 5 -
 $\bar{H} = 0.18'$
 $T = 1.2 \text{ sec}$
 $L = 6.8'$
 $R = 5''$

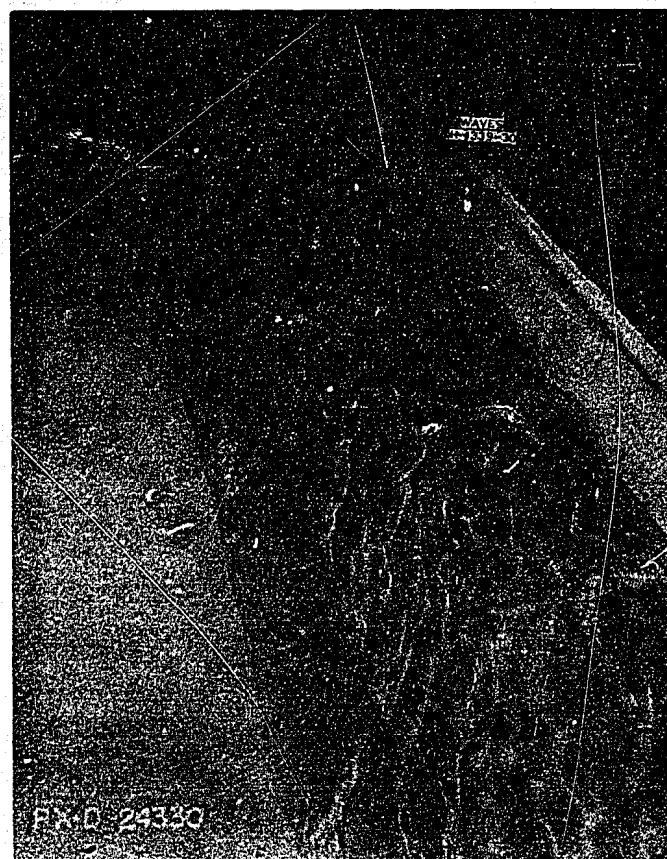


Hand-operated wave
generator used for
edge-wave demonstra-
tions.

FIGURE 21
Report Hyd 465

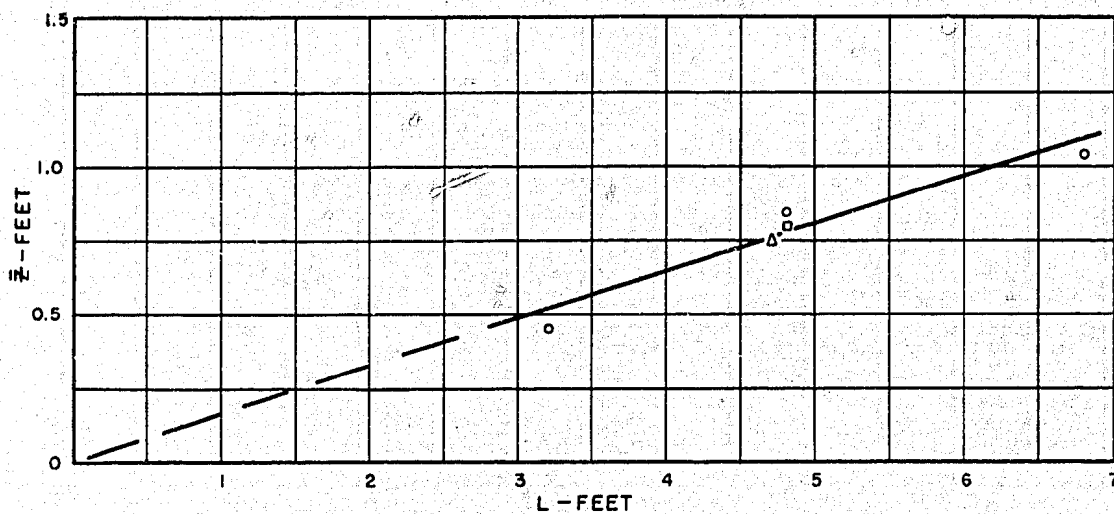


$L/y \approx 2.5$
Fairly well-defined
system of edge waves.
Edge wave 1/2 wave
length out of phase
with main wave.

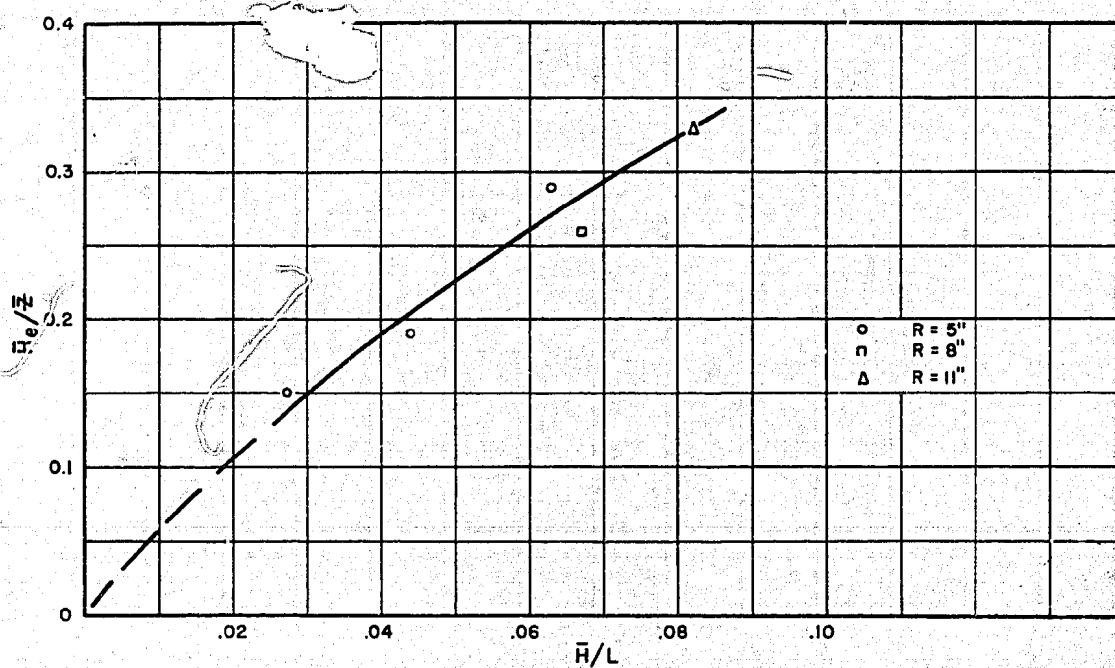


$L/y \approx 5$
Edge-wave system
not well defined.
Waves breaking
along slope, causing
wave front to move
diagonally across
channel.

EDGE-WAVE DEMONSTRATIONS

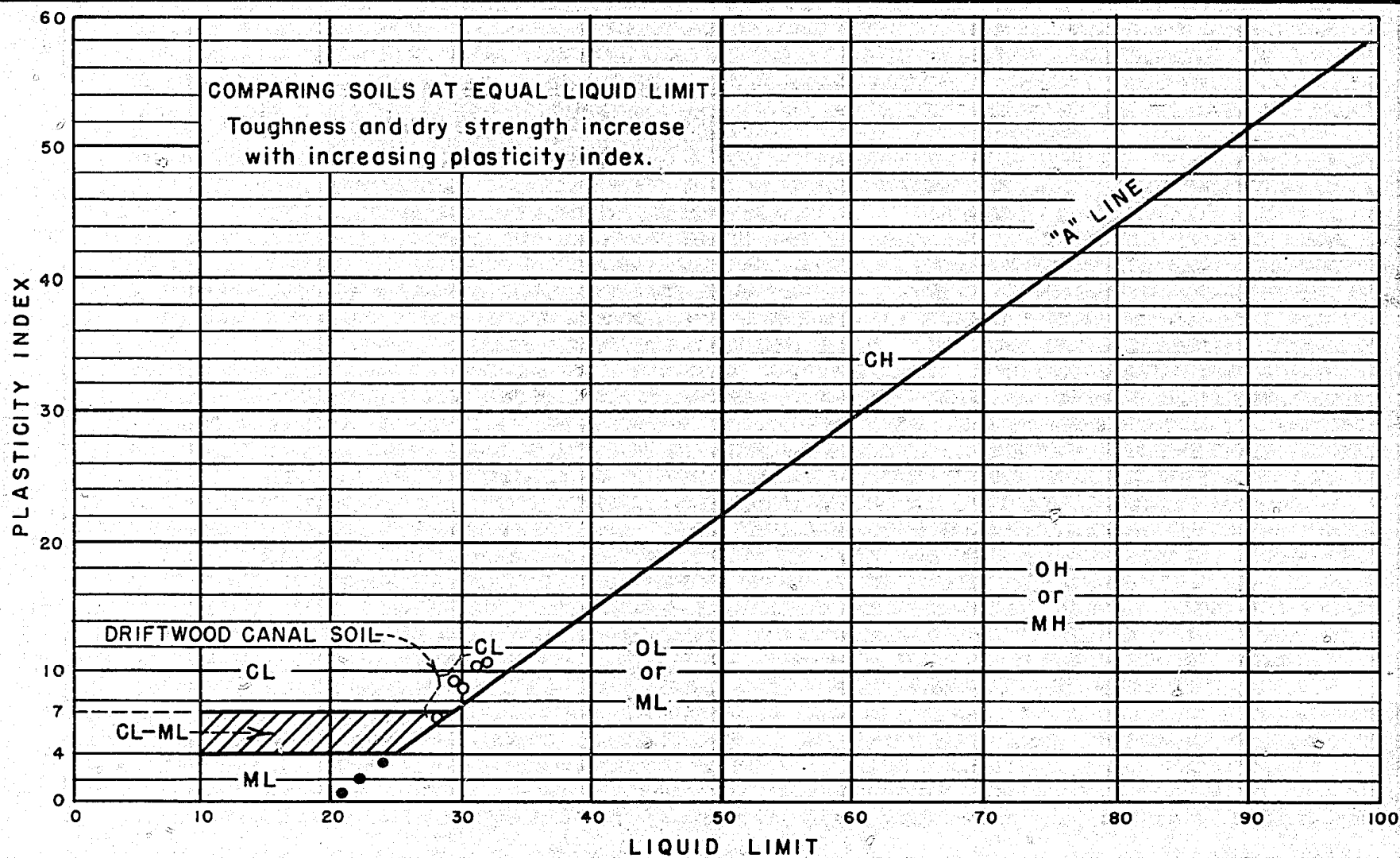


HORIZONTAL DISTANCE FROM EDGE-WAVE NODE
TO SLOPE (\bar{Z}) AS A FUNCTION OF WAVE LENGTH (L)



EDGE WAVE STEEPNESS (\bar{H}_0/\bar{Z}) AS A FUNCTION
OF WAVE STEEPNESS (\bar{H}/L)

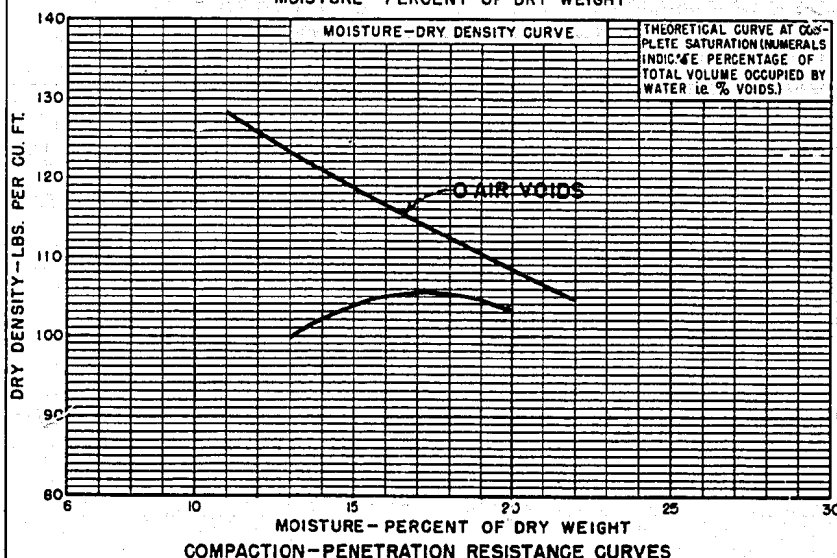
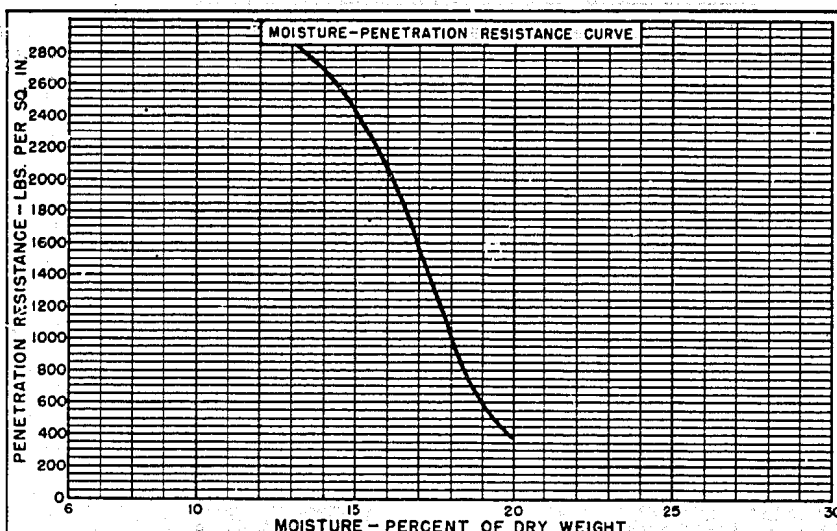
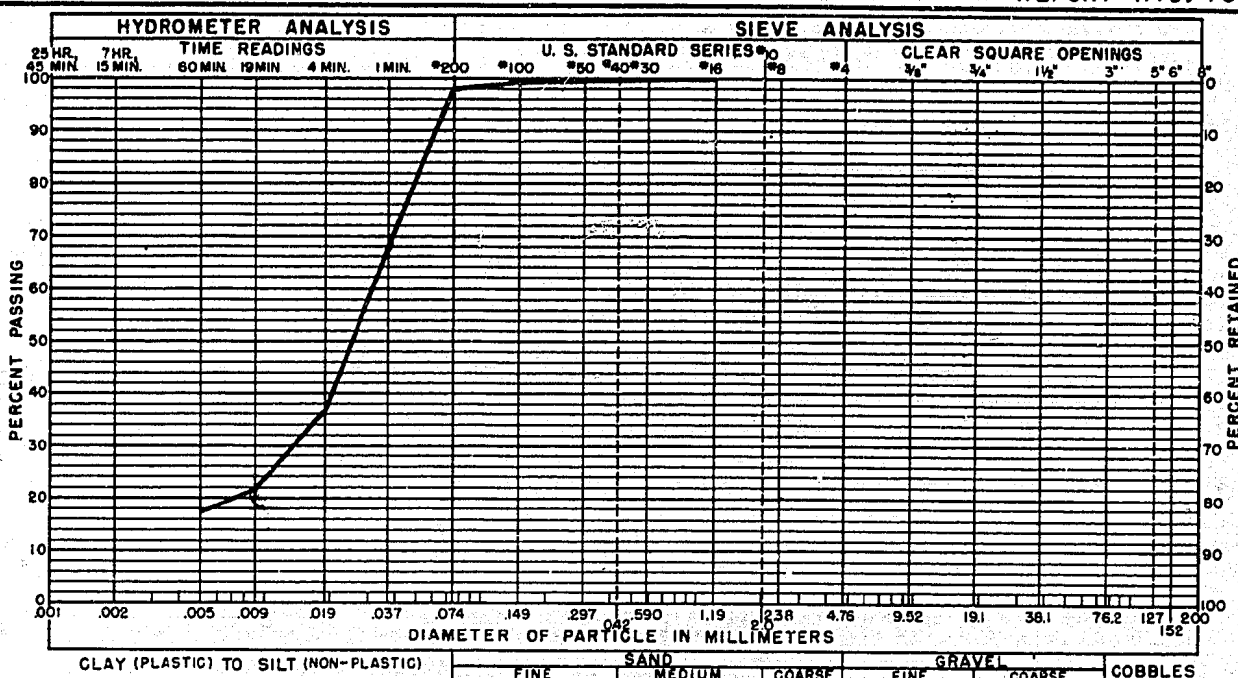
EDGE-WAVE RELATIONSHIPS



PLASTICITY CHART
FOR LABORATORY CLASSIFICATION OF FINE GRAINED SOILS

FIGURE 24
REPORT HYD. 465

STANDARD PROPERTIES SUMMARY



GRAVEL	0 %
SAND	1.8 %
SILT TO CLAY	98.2 %

STANDARD PROPERTIES SUMMARY

VISUAL CLASSIFICATION **CL**

SPECIFIC GRAVITY **2.659**

ATTERBERG LIMITS

LIQUID LIMIT **30.2**

PLASTICITY INDEX **9.2**

SHRINKAGE LIMIT

COMPACTION

% LARGER THAN TESTED

MAX. DRY DENSITY (P.C.F.) **105.4**

OPTIMUM MOIST. CONT. (%) **17.3**

PENETRATION RESIST. (P.S.I.) **1400**

PERCOLATION SETTLEMENT

PLACEMENT CONDITION

PERMEABILITY (FT./YR.)

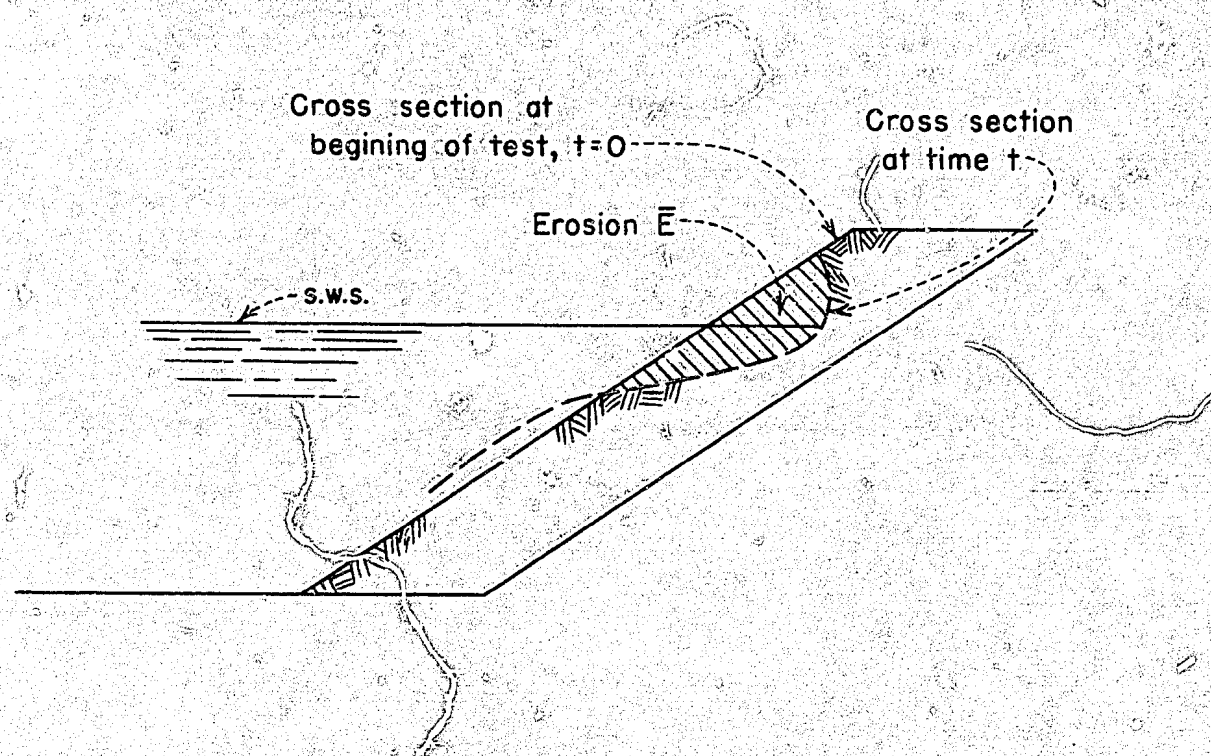
SETTLEMENT (%) UNDER

P.S.I. LOAD

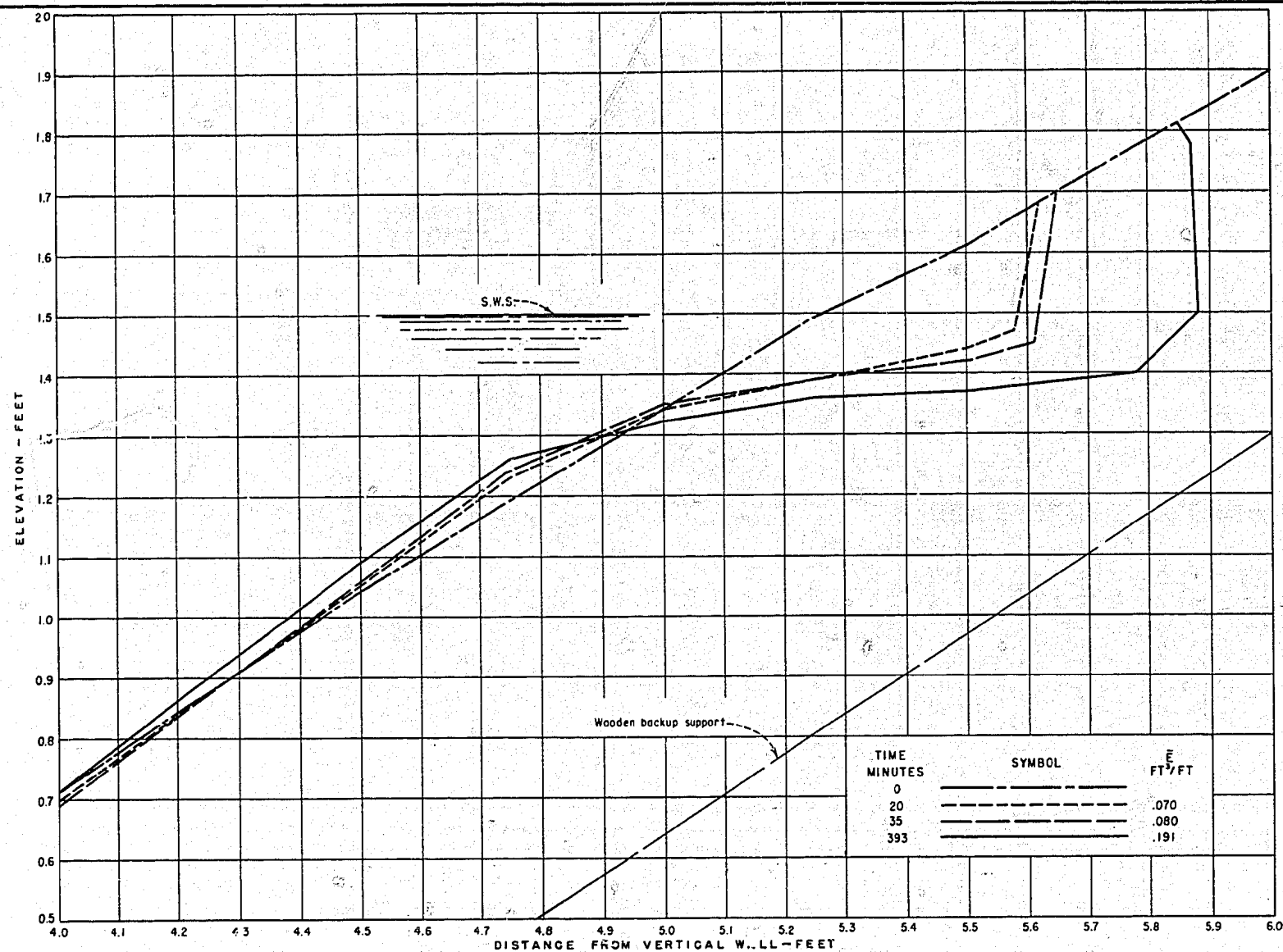
NOTES: Average results of tests performed on Drift-wood Canal soil used for wave studies.

STANDARD SOIL PROPERTIES

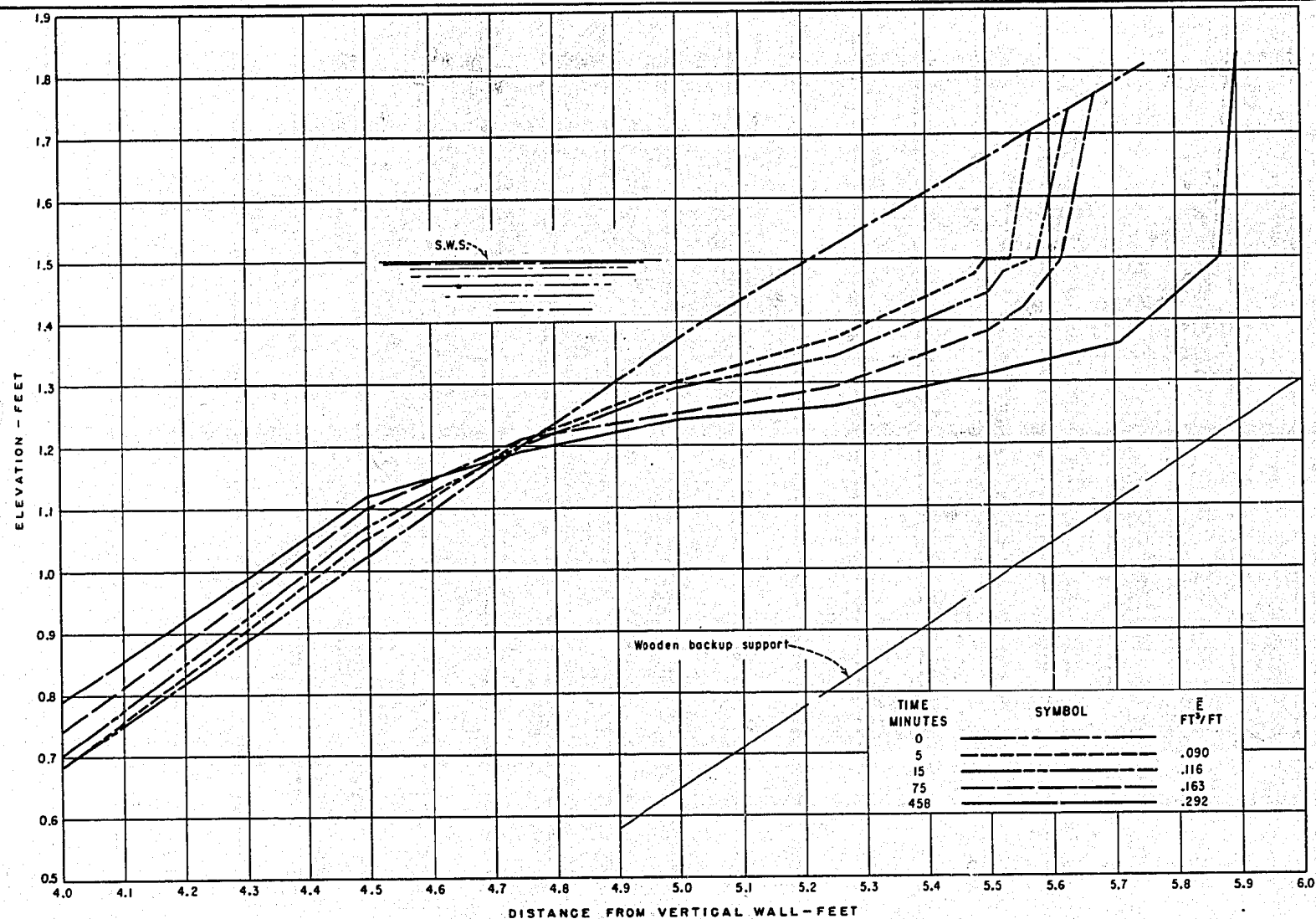
LABORATORY SAMPLE No. FIELD DESIGNATION EXCAVATION No. DEPTH FT.



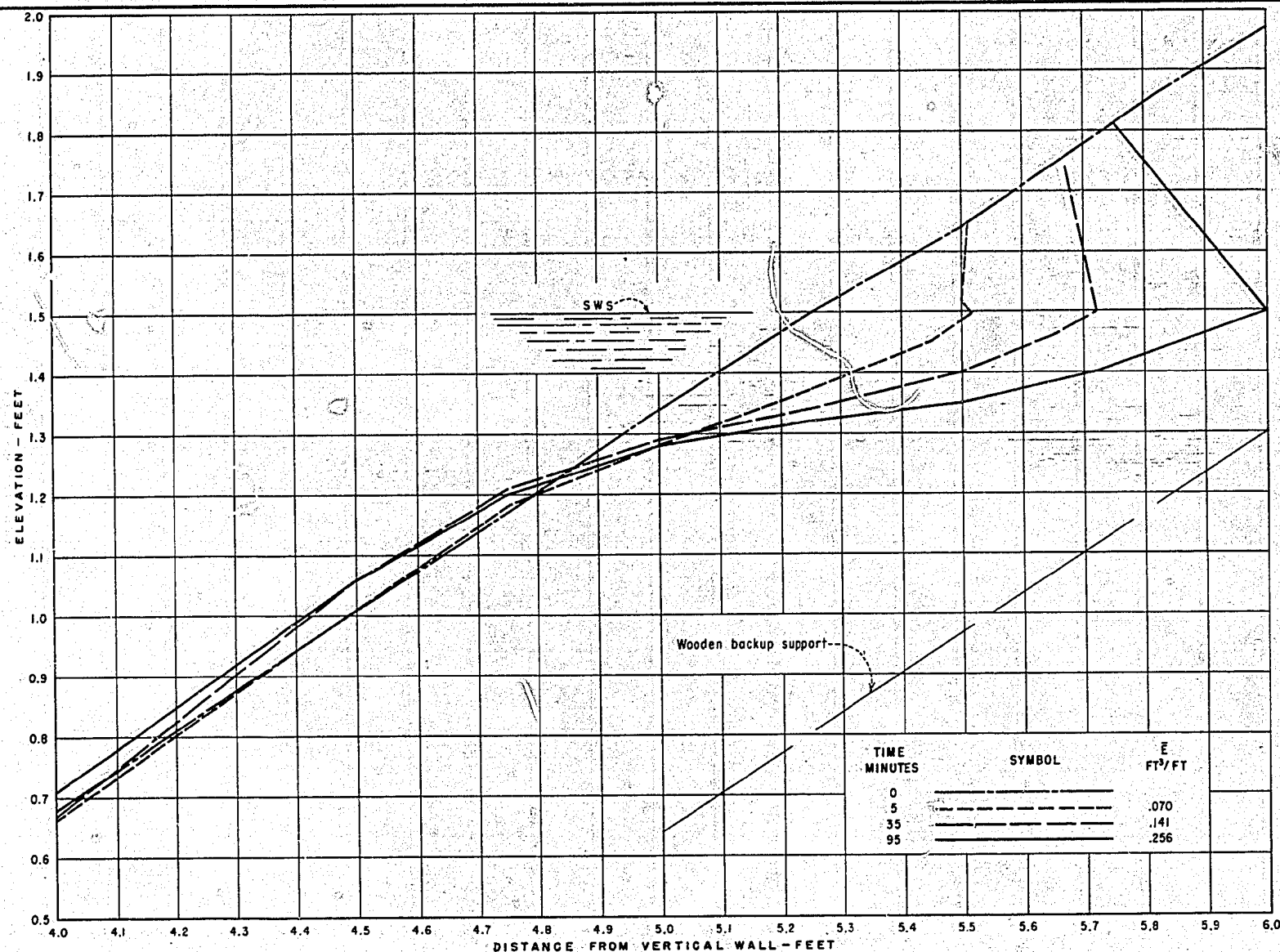
DEFINITION SKETCH OF EROSION IN TEST SECTION



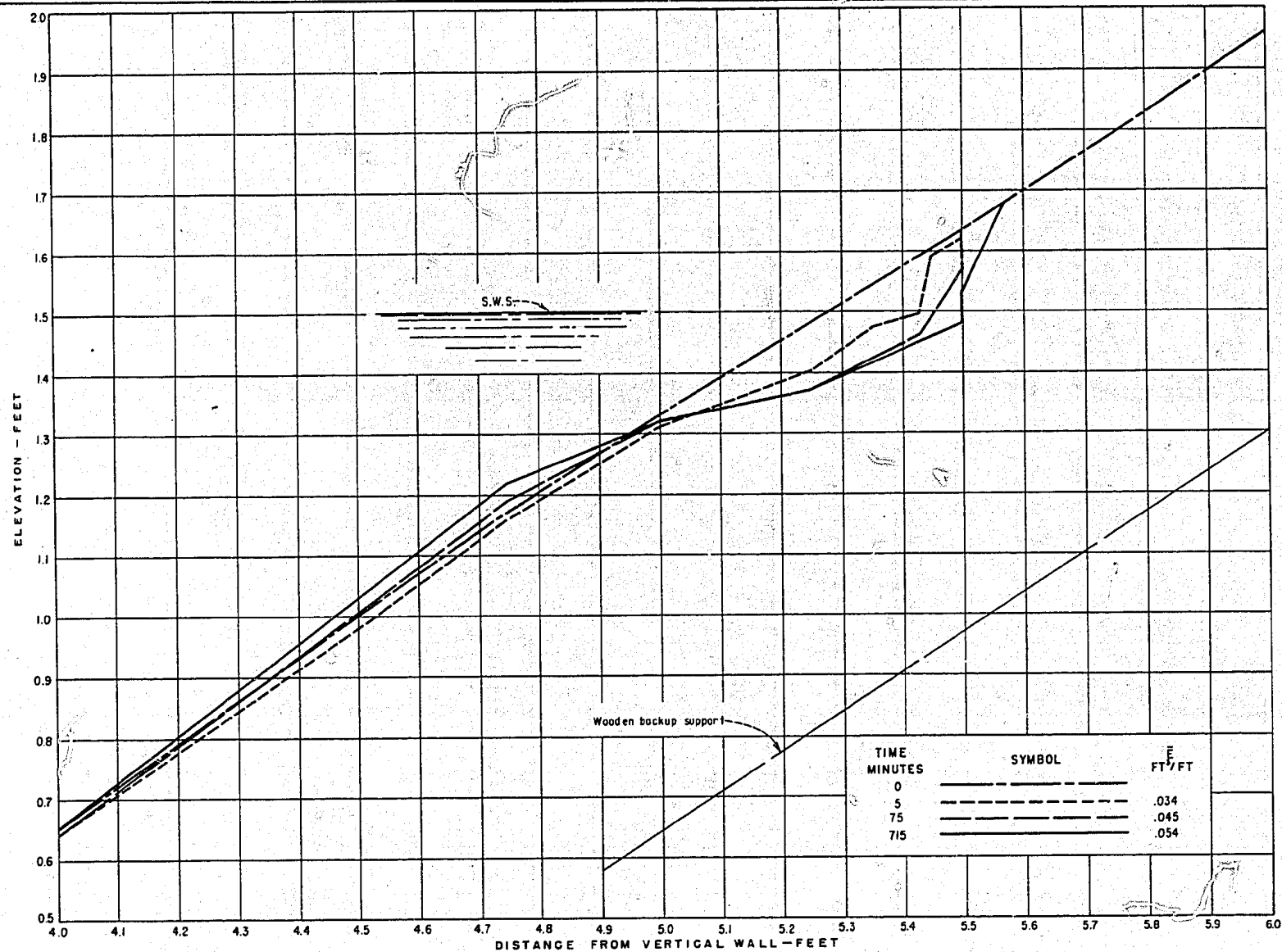
RUN 1-S - AVERAGE EROSION CROSS SECTIONS FOR MIDDLE 6' OF TEST SECTION



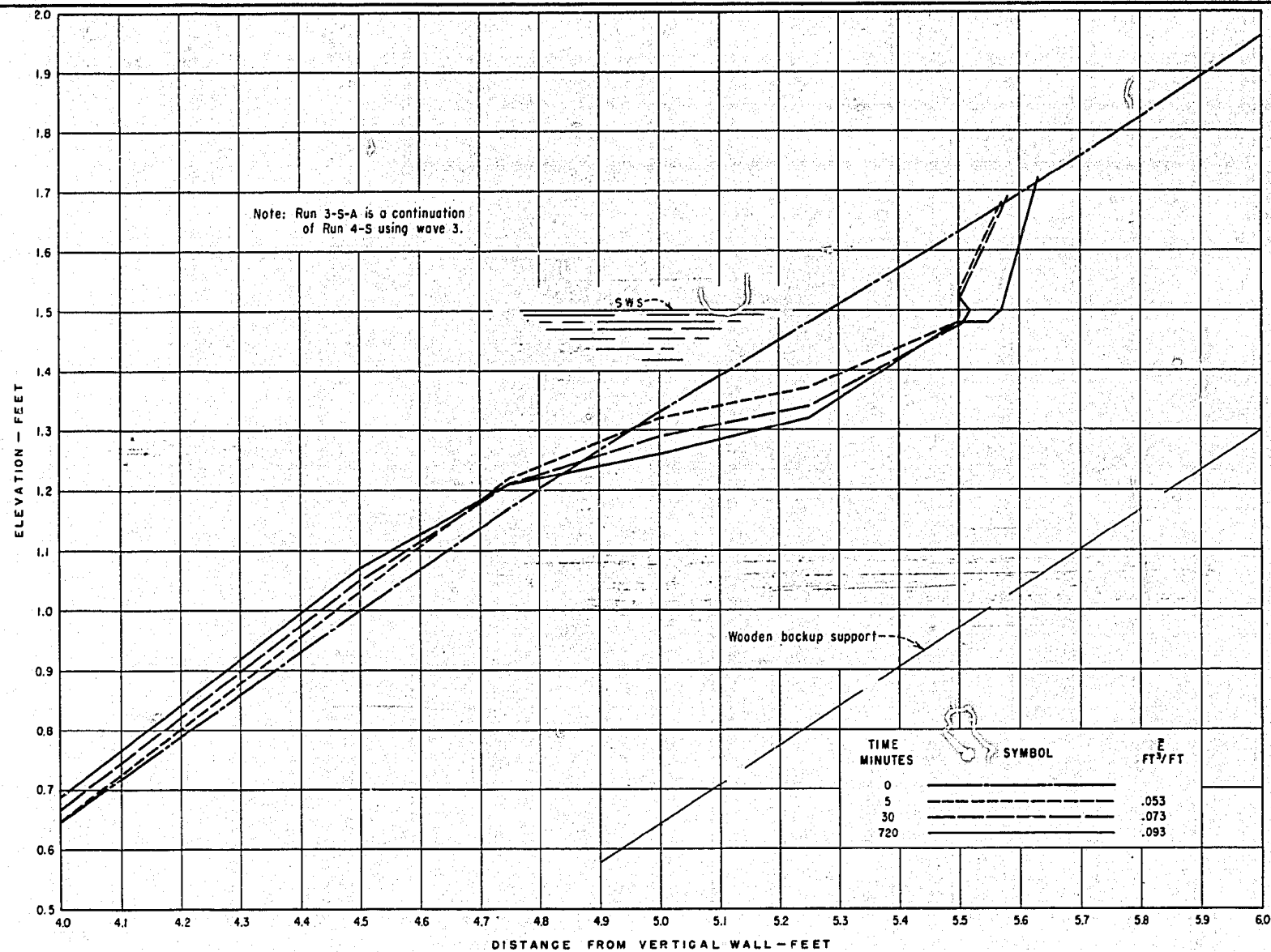
RUN 2-S - AVERAGE EROSION CROSS SECTIONS FOR MIDDLE 6' OF TEST SECTION



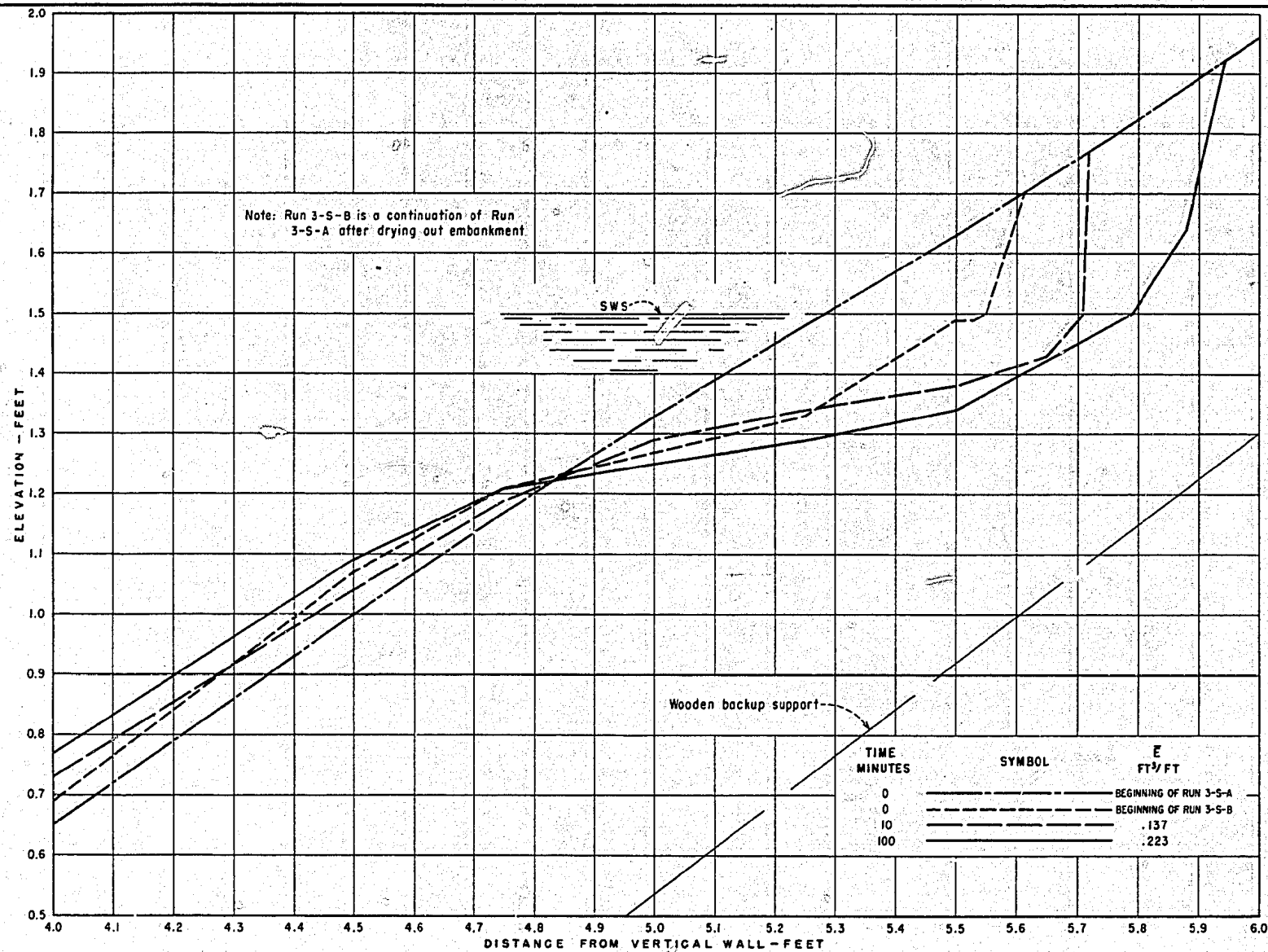
RUN 3-S - AVERAGE EROSION CROSS SECTIONS FOR MIDDLE 6' OF TEST SECTION



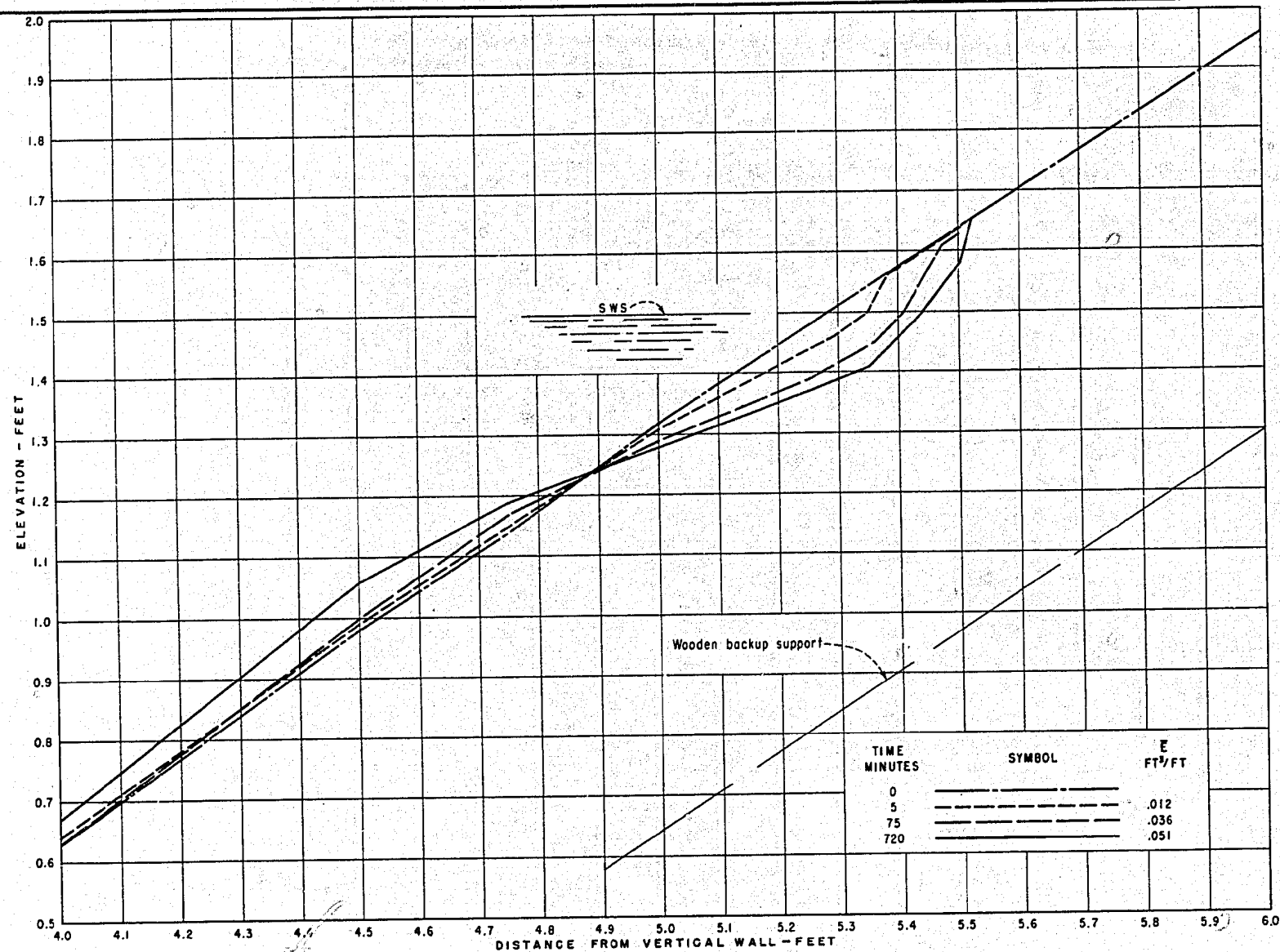
RUN 4-S - AVERAGE EROSION CROSS SECTIONS FOR MIDDLE 6' OF TEST SECTION



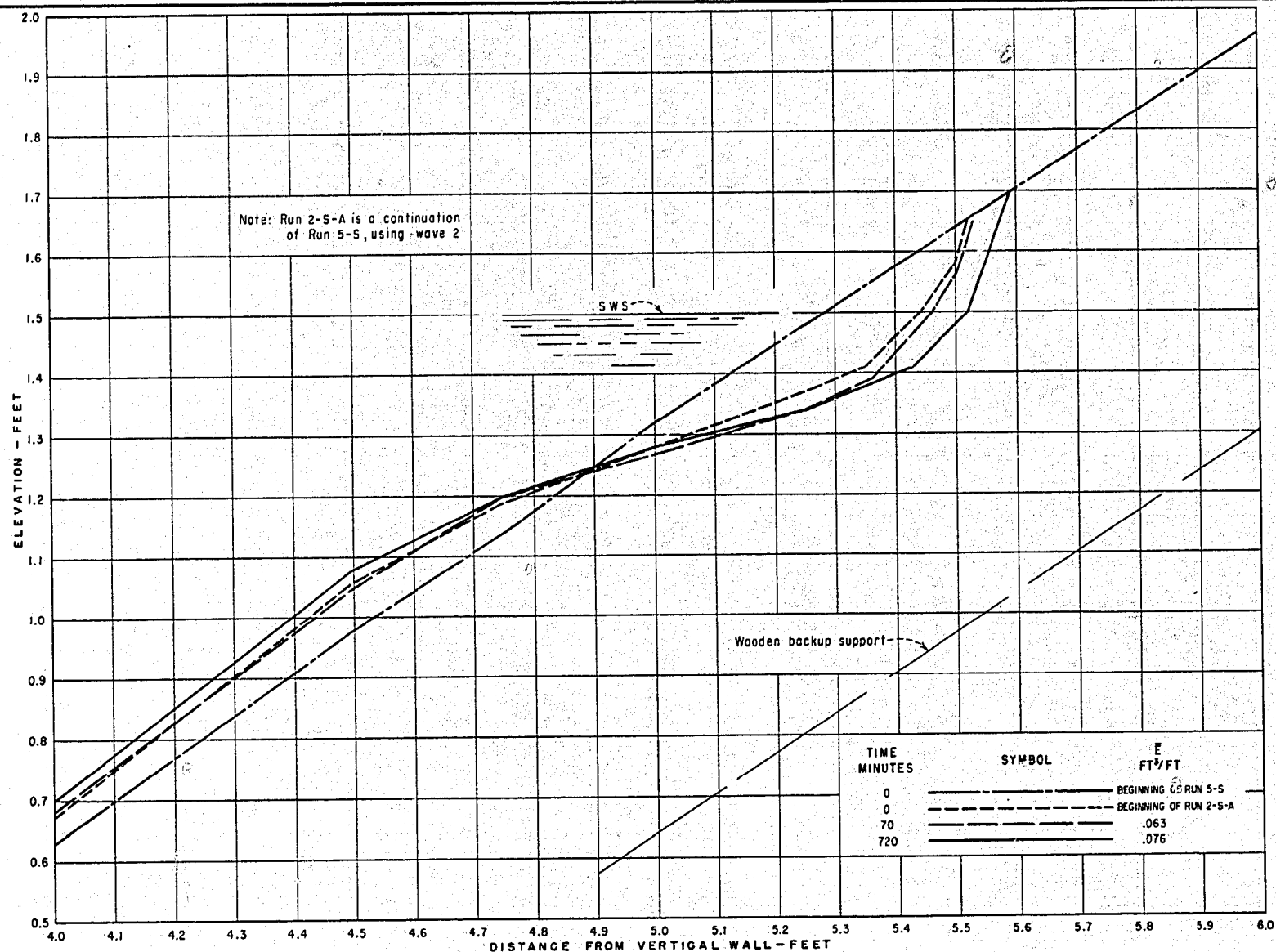
RUN 3-S-A - AVERAGE EROSION CROSS SECTIONS FOR MIDDLE 6' OF TEST SECTION



RUN 3-S-B - AVERAGE EROSION CROSS SECTIONS FOR MIDDLE 6' OF TEST SECTION



RUN 5-S - AVERAGE EROSION CROSS SECTIONS FOR MIDDLE 6' OF TEST SECTION



RUN 2-S-A - AVERAGE EROSION CROSS SECTIONS FOR MIDDLE 6' OF TEST SECTION



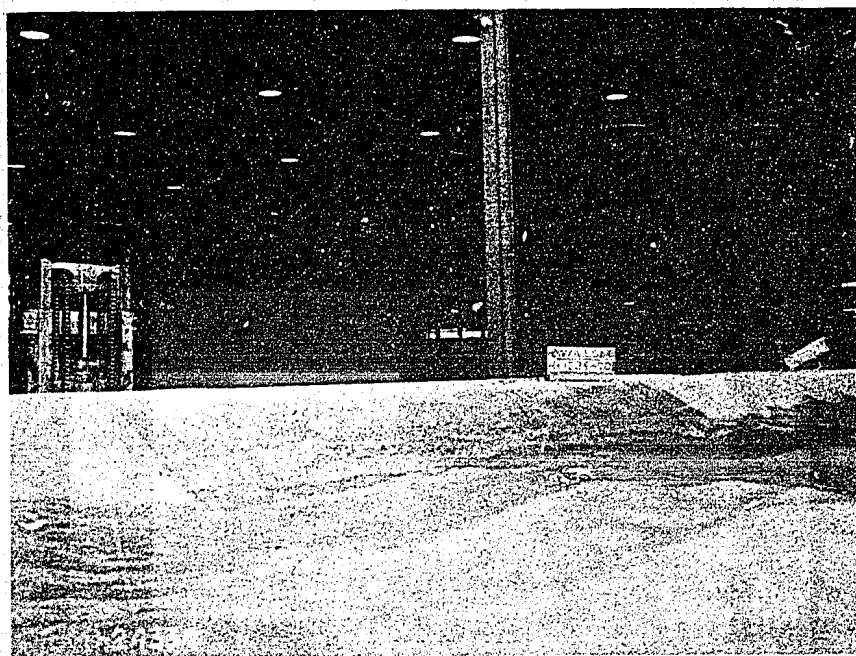
Run 1-S
 $t = \text{approx. } 6 \text{ hrs.}$



Test section after
Run 1-S
 $t = 6\frac{1}{2} \text{ hrs.}$



Run 2-S
t = approx. 3½ hrs.



Run 3-S
t = 25 min.

WAVE-EROSION TESTS - RUNS 2-S AND 3-S

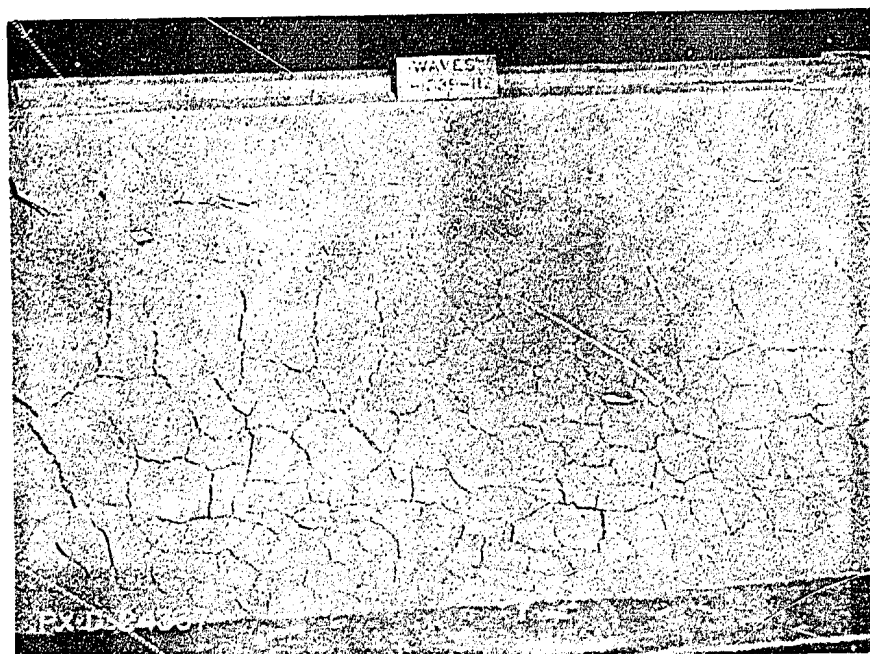


Run 4-S
 $t = \text{approx. } 4 \text{ hrs.}$

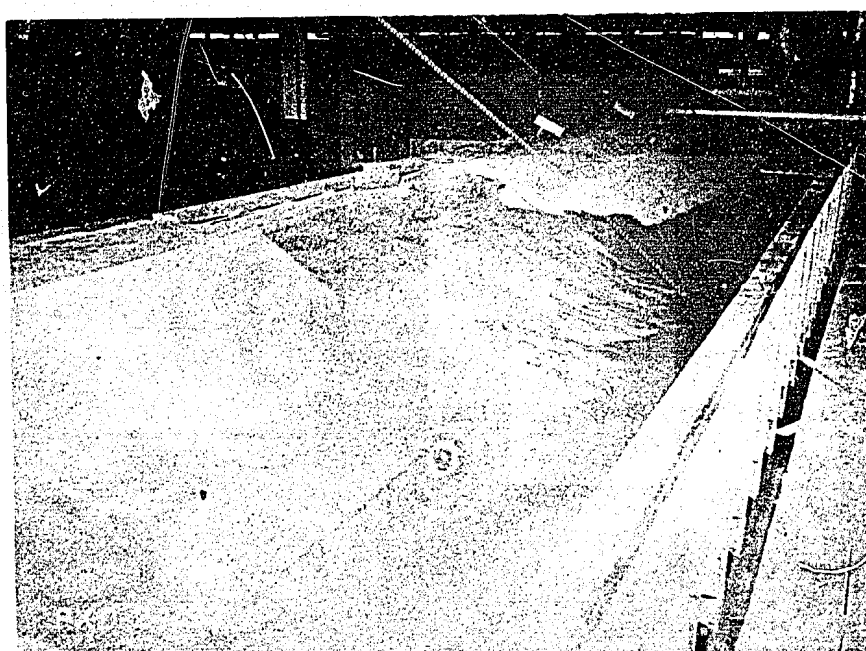


Run 3-S-A
 $t = \text{approx. } 5\frac{1}{2} \text{ hrs.}$

WAVE-EROSION TESTS - RUNS 4-S AND 3-S-A



Test section after
drying out prior to
Run 3-S-B.



Test section after
Run 3-S-B
 $t = 100$ min.

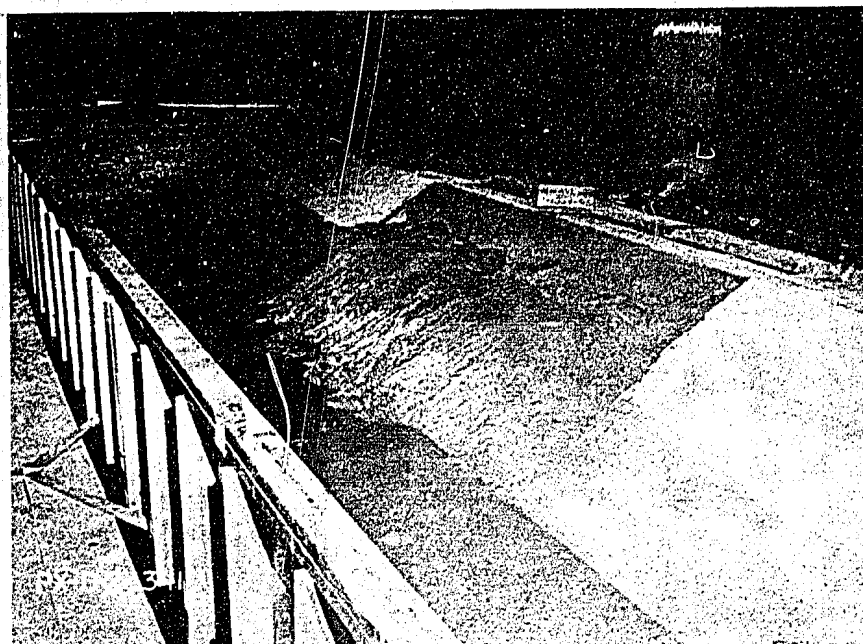
WAVE-EROSION TESTS - RUN 3-S-B



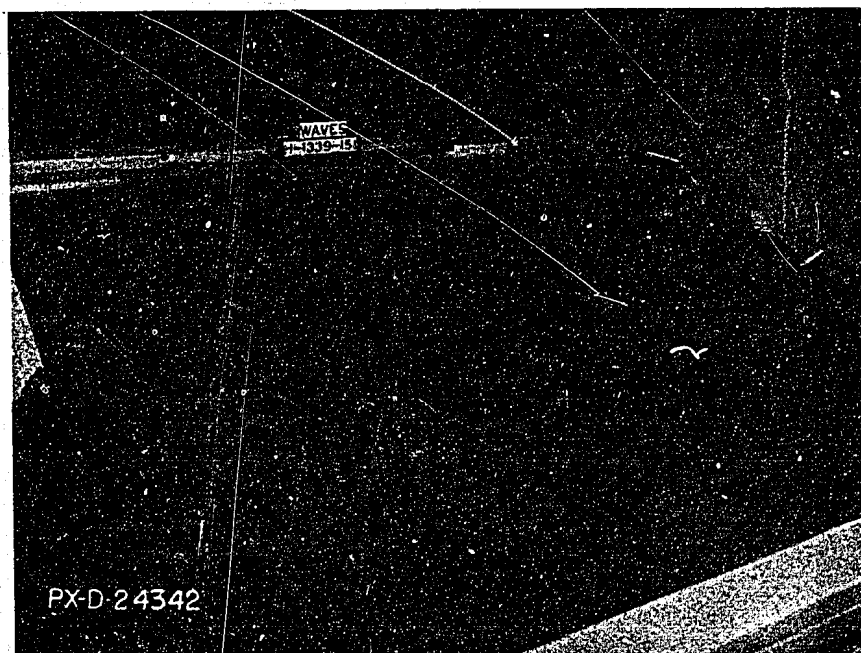
Run 5-S
t = approx. 10 hrs.



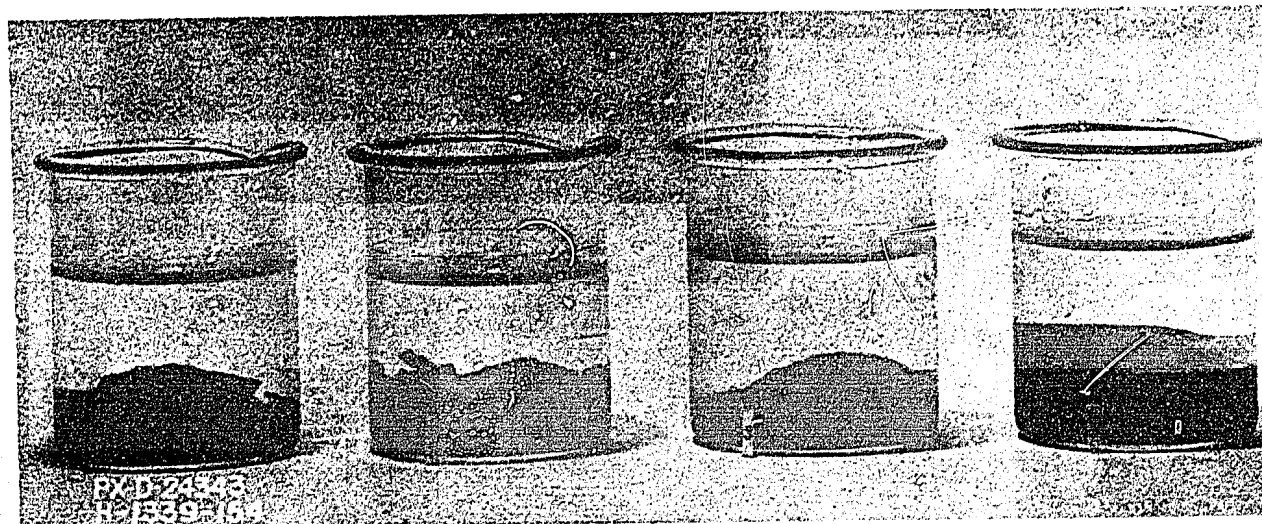
Run 2-S-A
t = approx. 8½ hrs.



Test section after
Run 4-S
 $t = 12$ hrs.

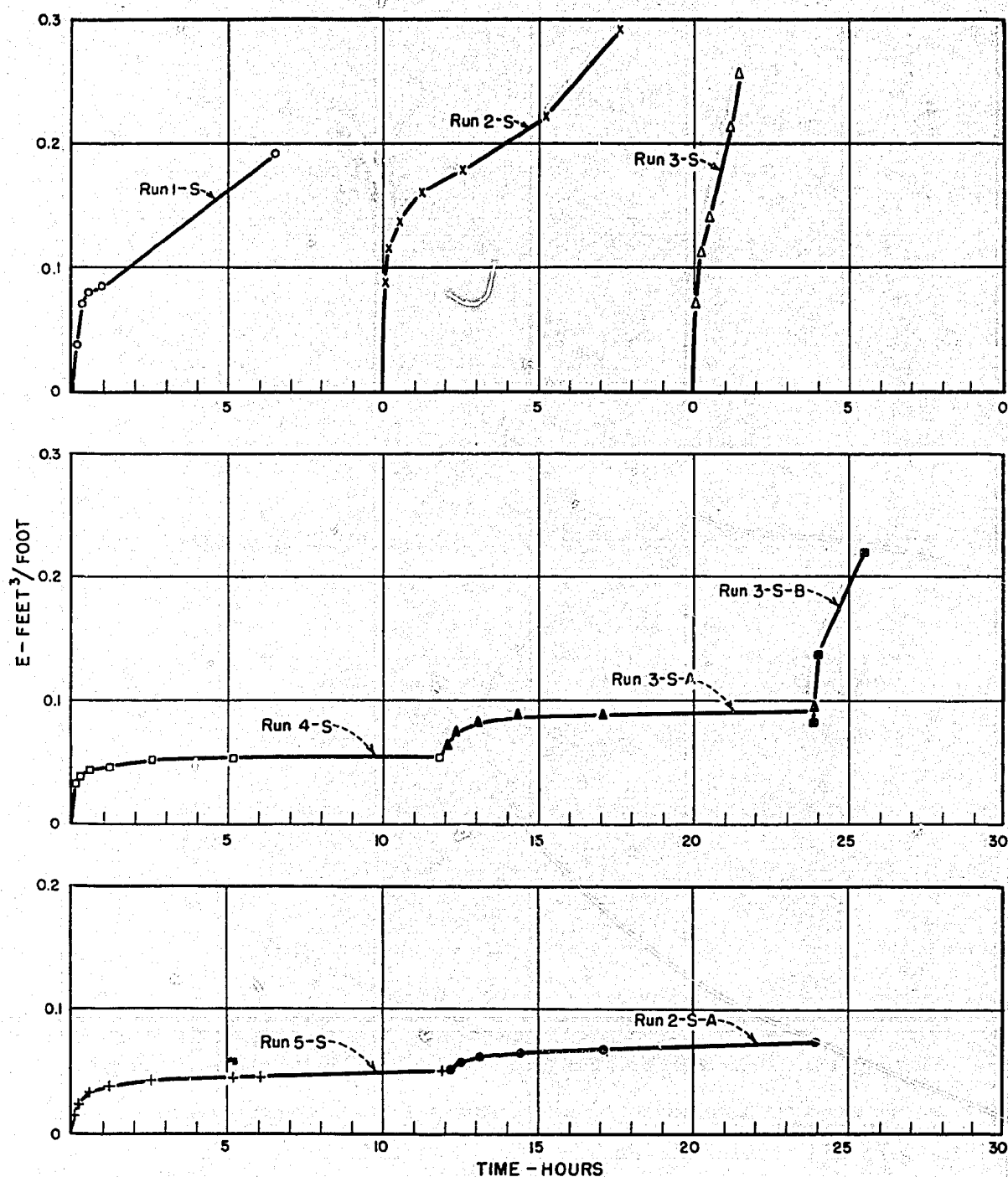


Test section after
Run 2-S-A
 $t = 12$ hrs.

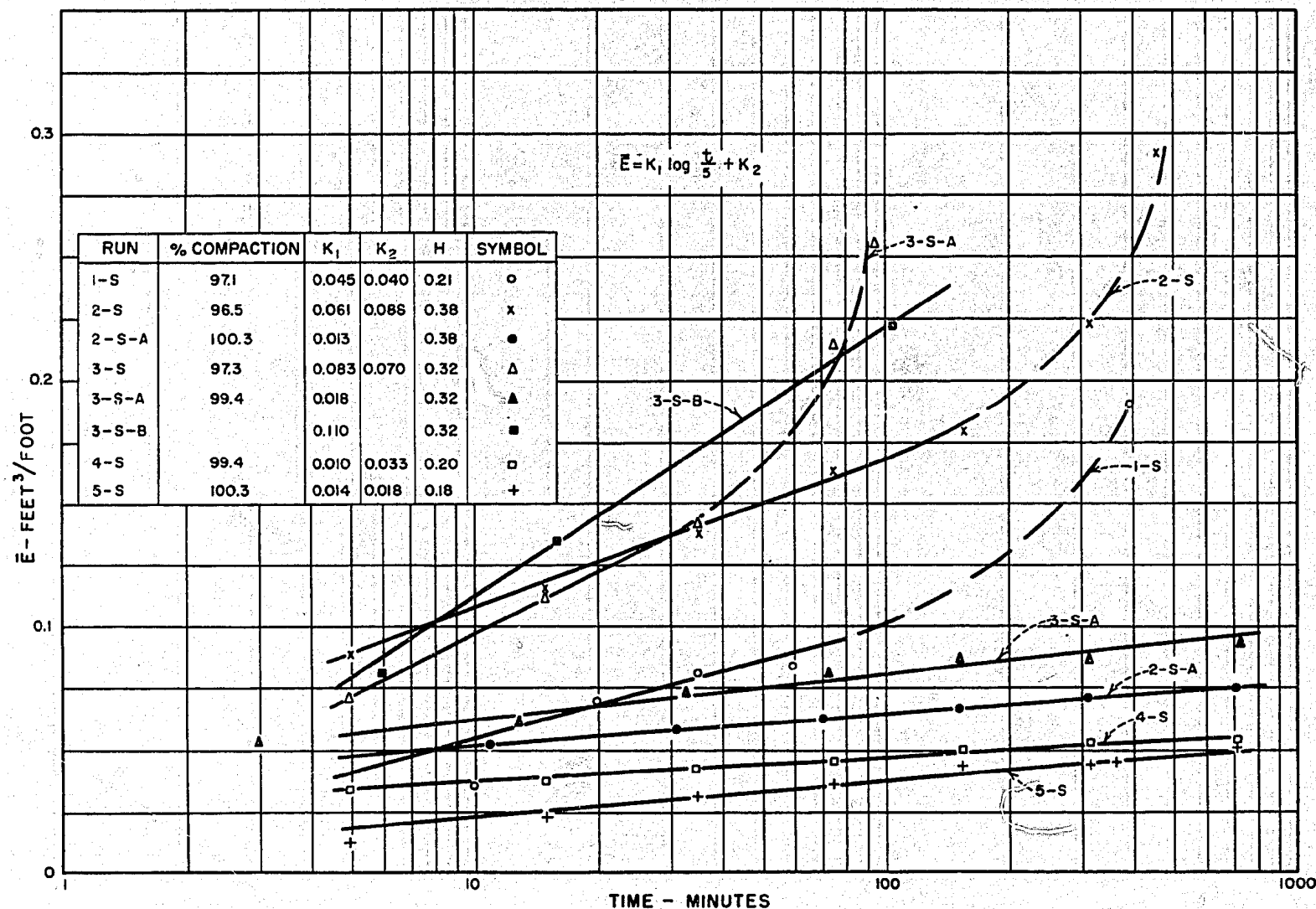


Beaker No.	Description
①	1/2 of loose clod taken from beach and placed in water immediately after draining flume. Flume drainage time approx. 18 hrs.
②	Clod placed in water immediately after draining and cutting from interior of moist embankment.
③	Other half of clod in Beaker No. 1. Placed in freezer for 3 days prior to immersion in water.
④	Clod taken from embankment and placed in water after embankment air dried for one week.

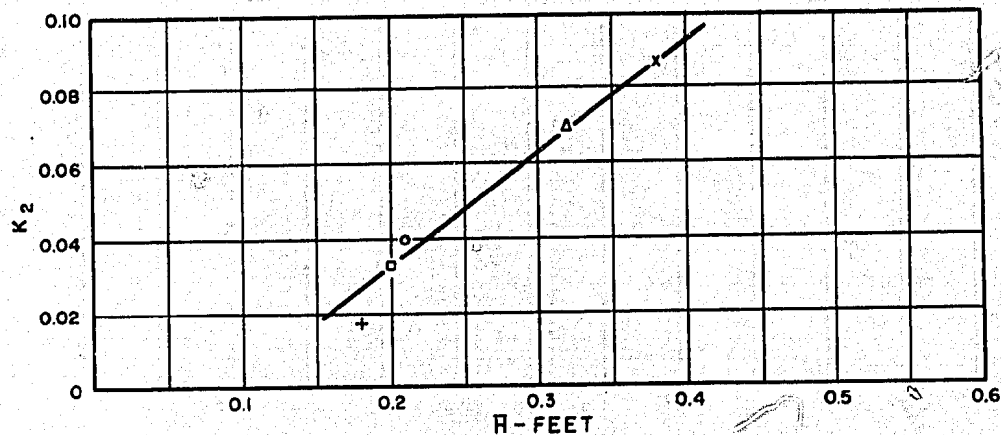
RESULTS OF WETTING- DRYING- FREEZING-
THAWING DEMONSTRATION



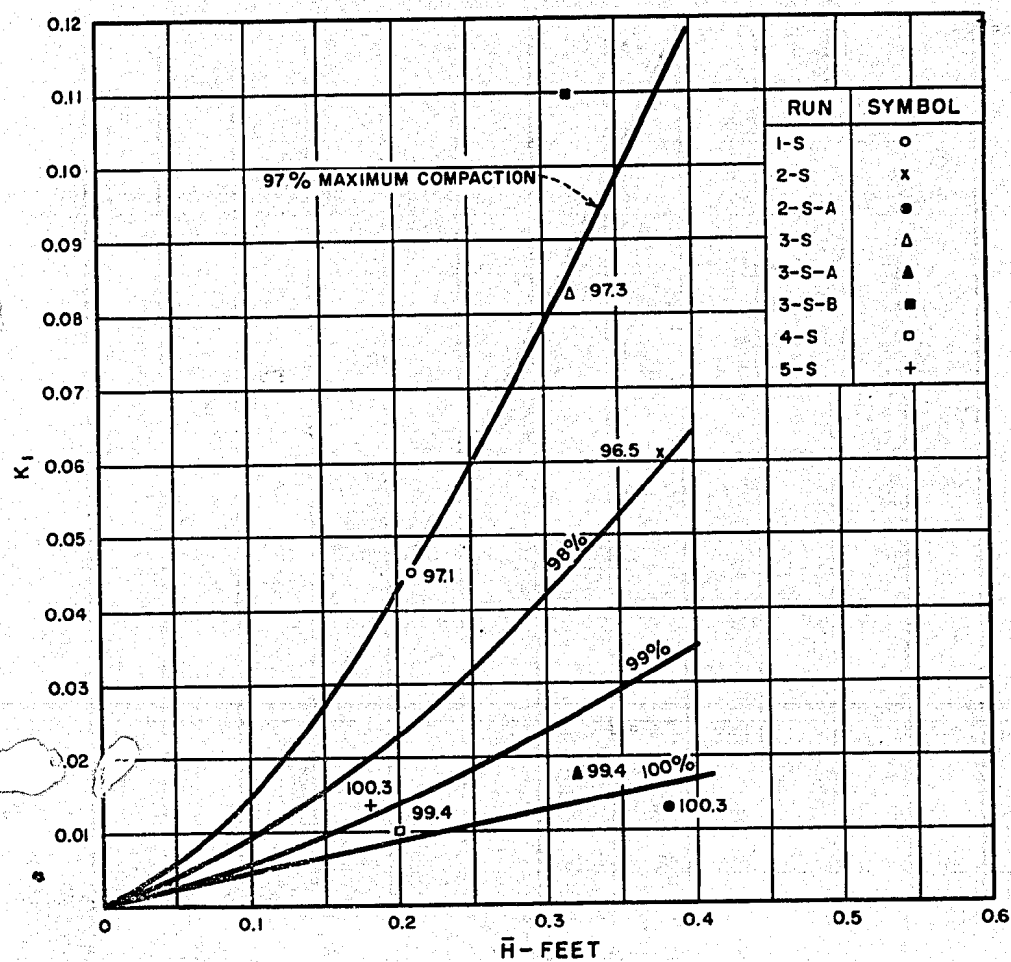
AVERAGE VOLUMETRIC DISPLACEMENT IN MIDDLE 6' OF
TEST SECTION AS A FUNCTION OF TIME



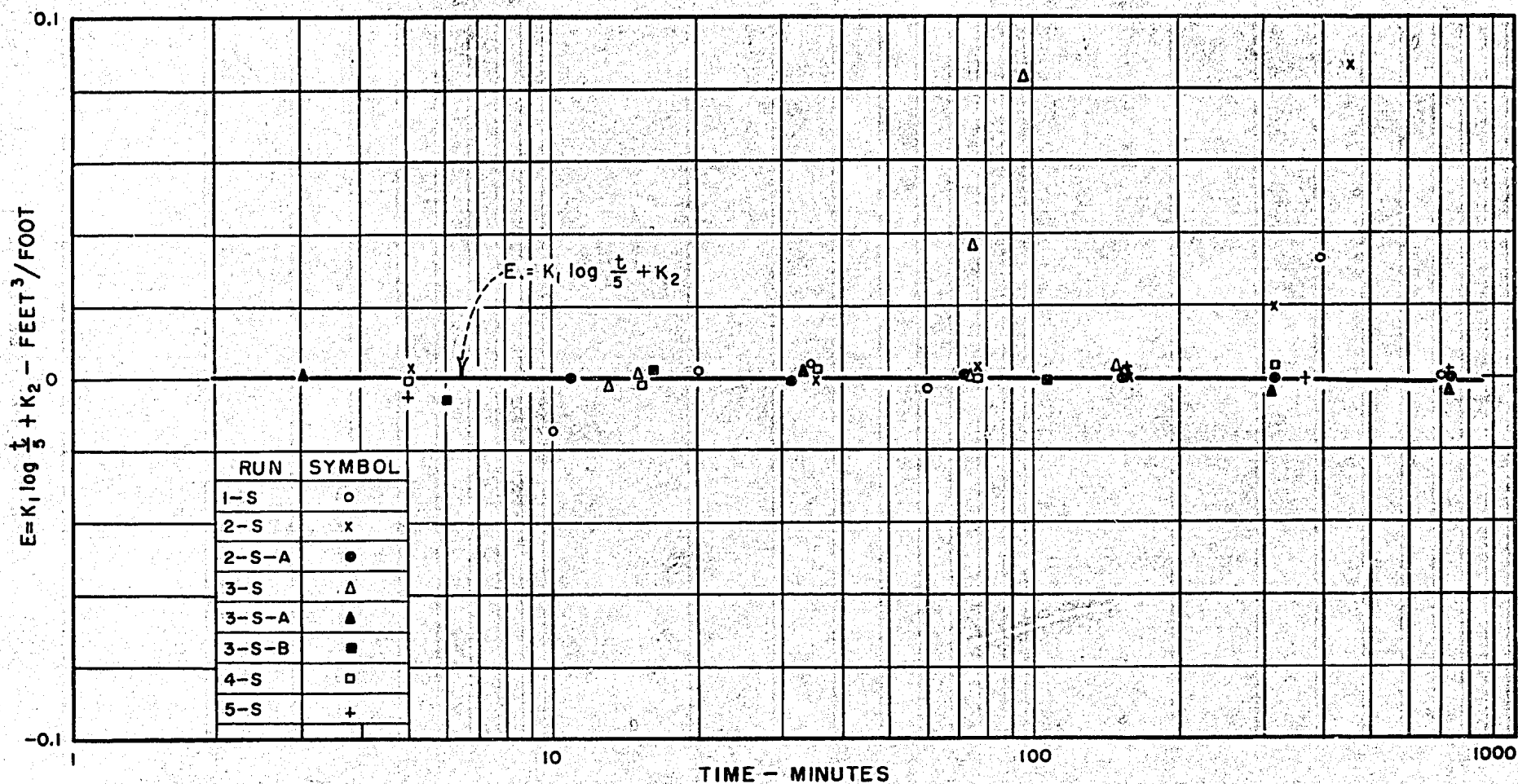
AVERAGE VOLUMETRIC DISPLACEMENT IN MIDDLE 6' OF
TEST SECTION AS A FUNCTION OF TIME



EMPIRICAL CONSTANT K_2 AS A
FUNCTION OF WAVE HEIGHT



EMPIRICAL CONSTANT K_1 AS A FUNCTION OF
WAVE HEIGHT AND % MAXIMUM COMPACTION



VOLUMETRIC DISPLACEMENT (\bar{E}) AS A FUNCTION OF TIME
AND EMPIRICAL CONSTANTS K_1 AND K_2